energies

MDPI

Article

A Novel Nonlinear Combined Forecasting System for Short-Term Load Forecasting

Chengshi Tian and Yan Hao *

School of Statistics, Dongbei University of Finance and Economics, Dalian 116025, China; tian_chengshi@dufe.edu.cn

* Correspondence: 220150331@seu.edu.cn; Tel.: +86-183-4083-0838

Received: 27 February 2018; Accepted: 19 March 2018; Published: 22 March 2018

Abstract: Short-term load forecasting plays an indispensable role in electric power systems, which is not only an extremely challenging task but also a concerning issue for all society due to complex nonlinearity characteristics. However, most previous combined forecasting models were based on optimizing weight coefficients to develop a linear combined forecasting model, while ignoring that the linear combined model only considers the contribution of the linear terms to improving the model's performance, which will lead to poor forecasting results because of the significance of the neglected and potential nonlinear terms. In this paper, a novel nonlinear combined forecasting system, which consists of three modules (improved data pre-processing module, forecasting module and the evaluation module) is developed for short-term load forecasting. Different from the simple data pre-processing of most previous studies, the improved data pre-processing module based on longitudinal data selection is successfully developed in this system, which further improves the effectiveness of data pre-processing and then enhances the final forecasting performance. Furthermore, the modified support vector machine is developed to integrate all the individual predictors and obtain the final prediction, which successfully overcomes the upper drawbacks of the linear combined model. Moreover, the evaluation module is incorporated to perform a scientific evaluation for the developed system. The half-hourly electrical load data from New South Wales are employed to verify the effectiveness of the developed forecasting system, and the results reveal that the developed nonlinear forecasting system can be employed in the dispatching and planning for smart grids.

Keywords: short-term load forecasting; nonlinear forecasting; forecasting performance; combined model

1. Introduction

Electrical load forecasting plays a pivotal role in electrical systems [1]. High-precision forecasting models can significantly improve power system management and provide effective information for economic operators [2]. If the forecasting error were to decrease by 1%, the operating costs would decrease by 10 million pounds [3]. However, inaccurate forecasting results can result in huge losses for electric power companies. Overestimated forecasts lead to extra cost production, while underestimated forecasts lead to issues in supplying sufficient electricity, which could in turn result in large power system losses [4]. Many severe blackout events have occurred that have deeply affected social production and people's lives. For example, on 14 August 2003, the U.S.–Canada power grid suffered a serious blackout event. This accident affected approximately 50 million people and generated huge losses amounting to billions of dollars [5,6]. Furthermore, Hunan Province, China in 2008, Europe in 2006 and India in 2012 were affected by blackout events [7]. Clearly, if an effective forecasting model were in place to provide an early warning prior to such events, timely measures could be taken to prevent their occurrence. However, electrical systems are affected by various factors, such as country policies, population growth and the social environment [8]. Therefore, the development of an accurate, simple, and robust forecasting model is meaningful for load forecasting.

In recent years, several methods have been developed to decrease electrical load prediction error. These methods can be broadly categorized into two groups, namely traditional and intelligent forecasting methods [9]. Traditional forecasting methods are widely used in load forecasting because they are simple to apply. These methods include regression models [10,11], the grey forecasting model (GM) [12], autoregressive moving average (ARMA) model [13], the autoregressive integrated moving average (ARIMA) model [14], the Kalman filtering (KF) method [15], etc. However, traditional forecasting methods cannot achieve sufficient accuracy for nonlinear load series [9].

Intelligent forecasting methods have been applied to improve model performance in nonlinear time series [16–18]. Many intelligent methods have been used to load time series because they can effectively solve complicated processes [19]. Moreover, intelligent methods are regarded as powerful tools for load forecasting problems owing to their accurate and robust forecasting levels [20]. With the improvement in intellectual algorithms, several intelligent prediction methods have been employed in power load prediction, such as fuzzy logic [21], artificial neural network (ANN) [22,23] and support vector machines (SVM) [24,25].

All these single forecasting models cannot achieve high precision on all occasions, because each model exhibits its own advantages and disadvantages [26]. To eliminate the weaknesses that are inhered in single models, many combined forecasting models have been proposed that are able to achieve desirable forecasting performance, which are regarded as the research direction for obtaining effective performance [27,28]. More specifically, the combined forecasting methods, as first noted by Bates and Granger [29], are developed to improve the forecasting performance by combining the advantages of each models. In recent years, different types of individual models have been integrated into load forecasting to decrease forecasting error. For example, Wang et al. [30] applied adaptive particle swarm optimization (PSO) to obtain the weight coefficients of a combined model based on the seasonal ARIMA, seasonal exponential smoothing and the weighted SVM in power load prediction. Similarly, Xiao et al. [31] developed a combined model that integrated several neural networks, incorporating the back propagation neural network (BPNN), radial basis function (RBF), generalized regression neural network (GRNN) and genetic-algorithm-optimized back propagation neural network (GABPNN) into load forecasting. Zhao et al. [32] proposed a novel combined model based on a high-order Markov chain to predict power consumption. Xiao et al. [33] developed a combined forecasting model for load forecasting, which employed an optimization method to obtain the weights of each individual model. Moreover, from the above literatures, it can be concluded that combined models exhibit preferable predictive performance compared to single models. Generally, the above-mentioned combined forecasting models have integrated individual models by means of linear combinations, denoted as linear combined model, which also cannot always achieve the promising forecasting results.

To the best of our knowledge, most previous studies proposed linear combined model to forecast electrical power load, which can enhance the forecasting effectiveness to some extent. However, there are still many defects in linear combined model which can be summarized: (1) The linear combined model only takes the linear terms into account with a fixed weight, ignoring the significance of the potential nonlinear term, which may cause decline of forecasting accuracy; (2) The linear combined model can lead to poor forecasting results when there is a strong nonlinear relationship between the individual predictor and final results.

With the above-mentioned analysis considered, the nonlinear combined method can be adapted to obtain the better performance than linear combined models. Since the middle of the 1990s, the SVM model has been widely used in many fields, such as vessel traffic flow forecasting [34], air quality early-warning [35], electrical load forecasting [6], etc. Especially, in the fields of electrical load forecasting, Hong et al. [36–38] developed a series of SVM-based model that integrates some advanced optimization algorithm, which obtains better forecasting performance than other compared models. Inspired by the outstanding studies of Hong et al., the authors find that the SVM has superiority in nonlinear time series forecasting and is powerful and simply implemented in application. Therefore, the modified SVM model is developed, which employs the advanced optimization algorithm to determine the parameters for further improving the forecasting performance. More specifically, the modified SVM model is employed as a nonlinear combined method to combine forecasters.

Therefore, with the limitations and strengths discussed above, a novel nonlinear combined forecasting system, based on improved data pre-processing module, the forecasting module, and the evaluation module, is developed in this study. More specifically, the data preprocessing module improved by longitudinal data selection is incorporated in the developed combined forecasting system to extract and identify the main feature of electrical power load data, which further enhance the effectiveness of data pre-processing and then enhance the final forecasting performance; the forecasting module, including individual forecasting models (BPNN, firefly-algorithm-optimized back propagation neural network (FABPNN), Elman neural network (ENN) and wavelet neural network (WNN)) and the combined model construction, performs multi-step forecasting for electrical power load with an effective forecasting performance, which can provide the basic information for scientific operations of electrical power system. More specifically, the modified support vector machine is developed to integrate all the individual predictors and obtain the final prediction, which successfully overcomes the upper drawbacks of linear combined model. Furthermore, the comprehensive evaluation module is an integral part of a complete forecasting system, which can verify the forecasting effectiveness from typical evaluation metric and statistical perspective. In summary, the developed nonlinear combined model takes full advantage of each components and ultimately achieves final success in electrical load forecasting.

The major contributions of this paper are as follows:

(1) **In this study, we develop a new nonlinear combined forecasting system that can integrate the merits of individual forecasting models to achieve higher forecasting accuracy and stability.** More specifically, the improved data pre-processing module based on longitudinal data selection is successfully proposed, which further enhance the effectiveness of data pre-processing and then improve the final forecasting performance. Moreover, the modified support vector machine is developed to integrate all the individual predictors and obtain the final prediction, which successfully overcomes the upper drawbacks of linear combined model.

(2) **The proposed combined forecasting system aims to achieve effective performance in multi-step electrical load forecasting.** Multi-step forecasting can effectively capture the dynamic behavior of electrical loads in the future, which is more beneficial to power systems than one-step forecasting. Thus, this study builds a combined forecasting system to achieve accurate results for multi-step electrical load forecasting, which will provide better basic for power system administration, load dispatch and energy transfer scheduling.

(3) **The superiority of the proposed nonlinear combined forecasting system is validated well in a real electrical power market.** The novel nonlinear combined forecasting displays its superiority compared with the individual forecasting model, and the prediction validity of the developed combined forecasting system demonstrates its superiority in electrical load forecasting compared with linear combined models and the benchmark model (ARIMA) as well. Therefore, the new developed forecasting system can be widely used in engineering application.

(4) **A more comprehensive evaluation is performed for further verifying the forecasting system's effectiveness and significance.** The results of Diebold–Mariano (DM) test and forecasting effectiveness reveal that the developed nonlinear combined forecasting system performs a higher degree of prediction accuracy than other comparison models and that it is significantly different from traditional forecasting models in terms of the level of prediction accuracy.

(5) **An insightful discussion is provided in this paper to further verify the forecasting effectiveness of the proposed system.** Four discussions are performed, which include the

significance of the proposed forecasting system, the comparison with linear combined models, the superiority of the optimization algorithm and the developed forecasting system's stability, which bridge the knowledge gap for the relevant studies, and provide more valuable analysis and information for electrical load forecasting.

The remainder of this paper is structured as follows. Section 2 illustrates the framework of the developed combined system. In Section 3, complete ensemble empirical mode decomposition with adaptive noise (CEEMDAN), individual forecasting models (the BPNN, FABPNN, ENN and WNN), the method of constructing the combined model and certain forecasting evaluation criteria are provided. Section 4 describes the results of three experiments. Further discussion is described in Section 5, and finally, a conclusion is provided in Section 6.

2. Framework of Proposed Nonlinear Combined Forecasting System

A new nonlinear combined forecasting system is developed that exhibits greater effectiveness in electrical load forecasting. It addresses the drawbacks of the individual models, which cannot always be optimal in any given case; in addition, it considers the contribution of nonlinear terms of individual forecasting models to improving the final forecasting performance compared with the linear combined model. The basic framework of the developed combined forecasting system is outlined as follows.

- Considering that uncertainty and randomness exist in raw electrical load series, the data pre-processing module improved by longitudinal data selection is employed during the first stage of electrical load forecasting to extract the primary features of the raw electrical load series.
- Four ANNs, namely BPNN, FABPNN, ENN and WNN, which are regarded as the individual forecasting models, are constructed to predict the filtered load time series. Then the combination forecasting is constructed based on modified SVM, which is used to combine the forecasting results obtained by the BPNN, FABPNN, ENN and WNN.
- The prediction performance of the developed forecasting system is evaluated by employing typical accurate metrics, the Diebold–Mariano (DM) test and forecasting effectiveness.
- Multi-step forecasting is applied in order to further test the forecasting abilities of the proposed combined forecasting system. Multi-step forecasting is an extrapolation process for realizing forecasting values by means of historical data and previous forecasting values. The multi-step forecasting process is as follows:

  (a) 1-step forecasting: on the basis of the historical data $\{v(1), v(2), v(3), \ldots, v(M)\}$, the predicted data $\hat{v}(M+1)$ is acquired, where M is the sampled time of the data sequence.
  (b) 2-step forecasting: on the basis of the historical data $\{v(2), v(3), v(4), \ldots, v(M)\}$ and previously predicted value $\hat{v}(M+1)$, the predicted data $\hat{v}(M+2)$ is acquired.
  (c) 3-step forecasting: on the basis of the historical data $\{v(3), v(4), \ldots, v(M)\}$ and previously predicted value $\{\hat{v}(M+1), \hat{v}(M+2)\}$, the predicted data $\hat{v}(M+3)$ is acquired.

3. Proposed Combined Forecasting System

To obtain high-precision forecasting results, the developed nonlinear combined forecasting system includes three modules: data pre-processing, forecasting and evaluation module. Figure 1 depicts the flowchart of the proposed forecasting system. The main procedure how the developed forecasting system is working in electrical load forecasting mainly include: first, the improved data pre-processing module based on longitudinal data selection is successfully developed to eliminate the negative effects of noise, which seems to be a promising technique to extract and identify the main feature of electrical power load data, as shown in Figure 1 part I; second, the structure of input-output for modeling is shown in Figure 1 part II; third, four individual forecasters are provided to forecast future changes of electrical load data, as shown in Figure 1 part III; and then, as shown in Figure 1 part IV, the modified SVM model is developed as a nonlinear combined method to combine all forecasters and obtain the final forecasting result; Finally, as shown in Figure 1 part V, the comprehensive evaluation module is used to verify the forecasting effectiveness from typical evaluation metric and statistical perspective. The details of each module are presented as follows.

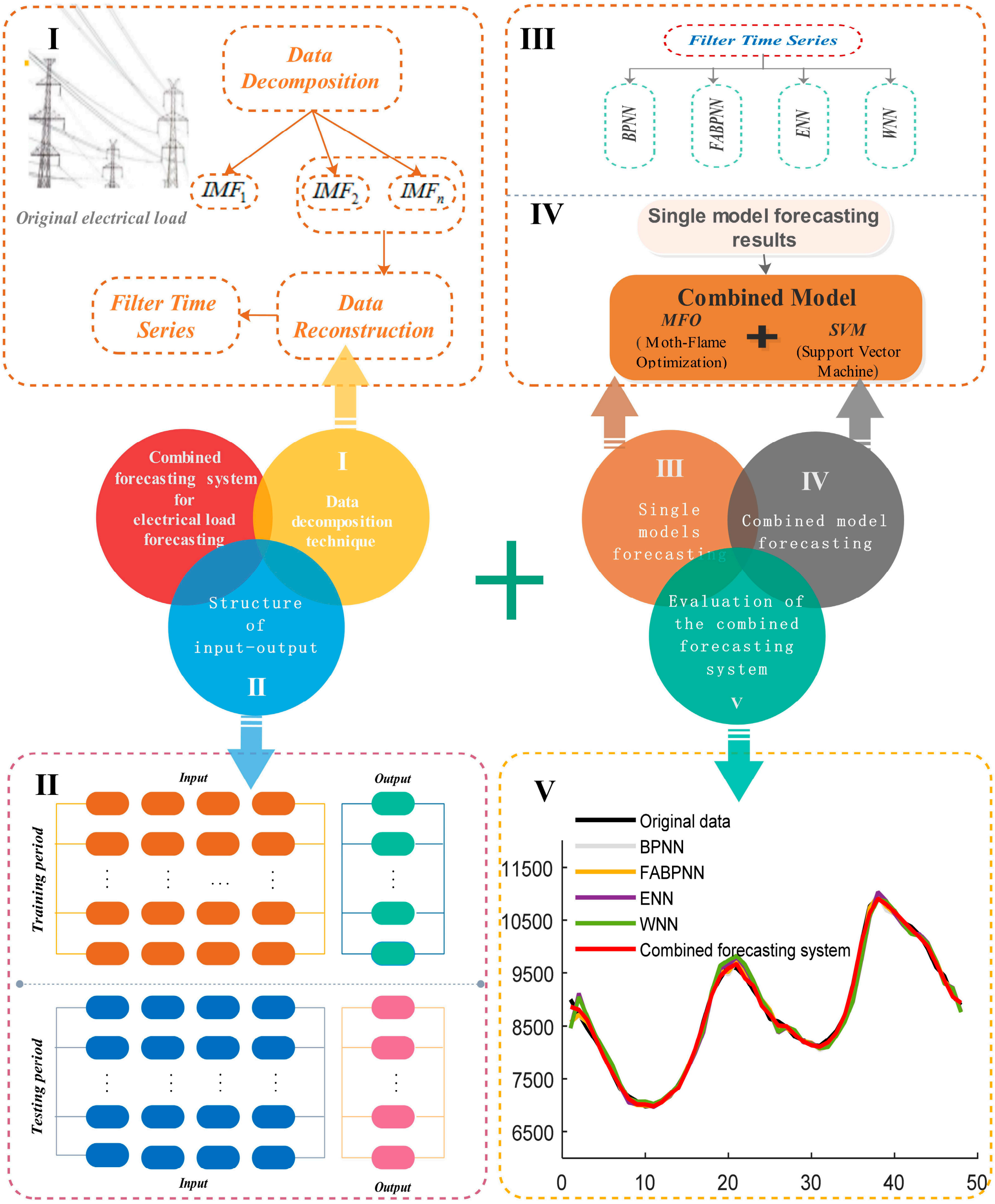

Figure 1. Flowchart of the proposed combined forecasting system.

3.1. Module 1: Improved Data Pre-Processing Module

Huang et al. [39] developed the empirical mode decomposition (EMD) technique, which can be employed to resolve the original sequences into intrinsic mode functions (IMFs). EMD can analyze complex data, such as non-stationary data, and many studies [40–42] successfully used EMD method in electrical load forecasting. However, it exhibits the defect of mode mixing, then the ensemble empirical mode decomposition (EEMD) method [43] has been developed to solve this defect. However, EEMD introduces two additional difficulties: residual noise exists in the reconstructed signal and the quantities of IMFs are likely to differ with the same decomposition. To address the mode mixing problem while maintaining the capacity to solve these additional difficulties, CEEMDAN was developed [44], and its main steps are illustrated in Figure 2 part A. Compared to EEMD, the main distinction of CEEMDAN is the introduction of adaptive noise. Therefore, this work employs the CEEMDN algorithm for data pre-processing. Several studies [45,46] have confirmed the successful application of CEEMDAN in the component filtering field. However, most previous studies only focused on conducting a simple data pre-processing, while ignoring the significance of data selection, which leaves much to be desired. Therefore, the improved data pre-processing module based on longitudinal data selection is successfully proposed, which further enhance the effectiveness of data pre-processing and then improve the final forecasting performance.

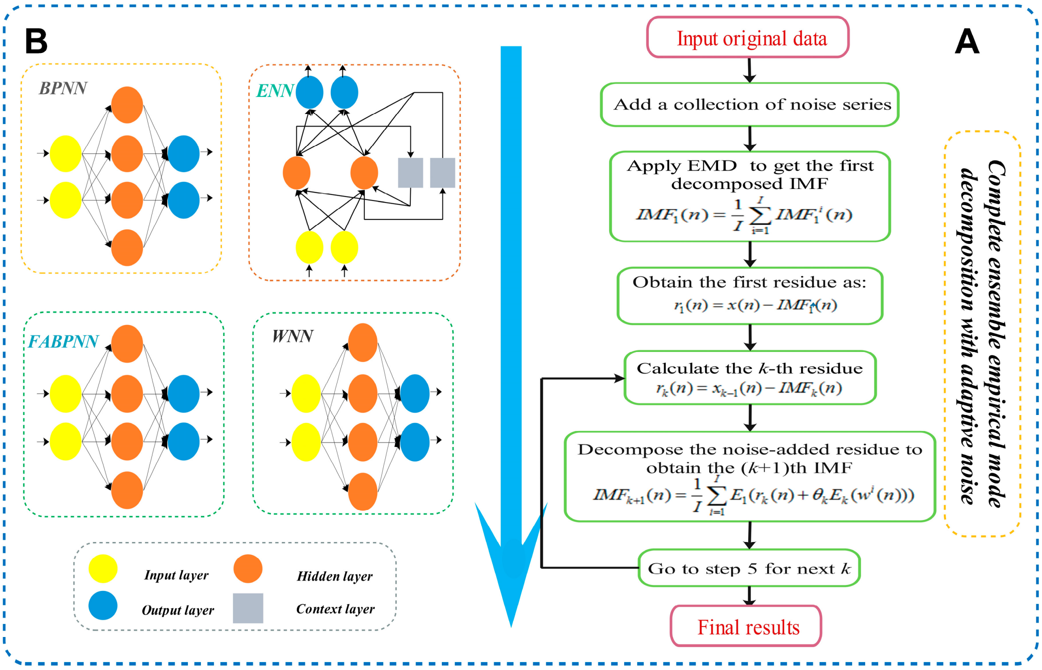

Figure 2. Structure of the individual models and complete ensemble empirical mode decomposition with adaptive noise (CEEMDAN). (**A**) Structure of the complete ensemble empirical mode decomposition with adaptive noise. (**B**) Structure of the individual models.

3.2. Module 2: Forecasting Module

3.2.1. Individual Forecasting Models

A variety of individual models can be used to obtain effective load forecasting performance. In this study, four widely used ANNs, namely the BPNN, FABPNN, ENN and WNN, are selected for the electrical load forecasting. The topological structure of the individual neural networks is depicted in Figure 2 part B.

Definition 1. *BPNN. There are two significant parameters in BPNN: weight and threshold. Suppose w_{ab} implies the weight connecting hidden node a and output node b, u_{bt} represents the weight connecting input node t and hidden node b, and $\hat{\theta}_b$ and θ_a display the threshold value of hidden node b and output node a, respectively. Then the output of hidden b: H_b can be calculated as:*

$$H_b = F(\sum_{t=1}^{T} u_{bt} I_t + \hat{\theta}_b) \tag{1}$$

where I_t is the input data of input node t, T denotes the input nodes' number, and F implies the S activation function which can be displayed as:

$$F(t) = \frac{1}{1+e^{-t}} \tag{2}$$

Then the output layer calculates the sum through:

$$O_a = \sum_{b=1}^{B} w_{ab} H_b + \theta_a \tag{3}$$

where B represents the hidden nodes' number.

Definition 2. *FABPNN. The FABPNN is a neural network model that mainly consists of two parts: firefly algorithm (FA) optimization and BPNN. More specifically, the thresholds and the weight values of BPNN are optimized by FA method. In addition, the detail description of FA algorithm can be found in [36].*

Definition 3. *ENN. The ENN model possess four layers: the input layer, the hidden layer, the context layer, and the output layer. Suppose the input data of neurons at time t is I_{it} (i = 1, 2, ... , r), the context layer neurons c_{vt} (v = 1, 2, ... , n) and net_{vt} (v = 1, 2, ... , n) at time t.*

The hidden layer neurons H_{vt} (v = 1, 2, ... , n) at time t can be displayed as:

$$H_{vt}(l) = F(net_{vt}(l)) = F(\sum_{i=1}^{r} w_{iv} I_{it}(l) + \sum_{v=1}^{n} s_v c_{vt}(l)) \tag{4}$$

where F is the hidden layer activation function which can be obtained by Equation (2), w_{iv} represents the weights connecting input layer node i and the hidden layer node v, and s_v is the weight between hidden layer node v and the context layer.

The output layer O_{t+1} is represented as follows:

$$O_{t+1}(l) = f(\sum_{v=1}^{n} k_v H_{vt}(l)) \tag{5}$$

where k_v is the weight between hidden layer node v and the output layer and f is an identity map as the activation function.

Definition 4. *WNN. Suppose the input data and output data in WNN are x_d (d = 1, 2, ... , g) and y_j (j = 1, 2, ... , l), separately. In addition, the output of hidden layer H is represented by:*

$$H(d) = H_d(\frac{\sum_{i=1}^{g} w_{id} x_d - q_d}{a_d}) \tag{6}$$

where H_d is the wavelet basis function, w_{id} is the weights connecting the input layer and hidden layer, q_d is the translation factor of the wavelet basis function, a_d represents the scaling factor of the wavelet basis function. Then the output is displayed as:

$$o(j) = \sum_{i=1}^{p} w_{ij} H(i), j = 1, 2, \ldots, l \tag{7}$$

where p represents the number of hidden node, and w_{ij} implies the weights connecting the output layer and hidden layer.

3.2.2. Combined Forecasting Model

The combination model is regarded as a promising method for acquiring prediction validity in load forecasting and can incorporate the advantages of the individual models.

The Theory of Combined Forecasting

Combined forecasting methods can be categorized as linear and nonlinear combined forecasting. The traditional linear combined method is represented as follows:

$$f = \sum_{t=1}^{d} w_t f_t \tag{8}$$

where w_t denotes the weight coefficient of the t-th prediction method, f_t is the forecasting result from the t-th prediction method, d is the quantity of single models, and f is the prediction result of the combined method. However, the linear prediction model offers limited applications, because it merely determines each model's influence, resulting in poor forecasting accuracy. The nonlinear combined method can successfully solve this problem of the linear combined model, as well as reducing uncertainty and taking full advantage of the information of each forecasting method. Meanwhile, it avoids computing the weight of the linear combined method. The nonlinear combined model is represented as follows:

$$f = \varphi(f_1, f_2, \ldots, f_d) \tag{9}$$

where f_t implies the prediction results of the t-th forecasting method, $\varphi(\ )$ is the nonlinear combined forecasting function, and f is the forecasted value of the nonlinear combined model.

Considering the strong nonlinear function mapping abilities of neural networks, we can implement an electrical load combination prediction method according to a neural network. However, owing to the generalization ability limitation, a neural network easily becomes trapped in the local optimal solution and cannot make full use of information by selecting a small sample [47]. Compared to traditional neural networks, the SVM seeks structural risk minimization and its two convex properties guarantee that a global optimal solution can be obtained. Therefore, the modified SVM is developed as a nonlinear combined method to combine all forecasters.

Support Vector Machine (SVM)

The SVM, developed by Vapnik [48,49], exhibits extensive application in nonlinear regression estimation, which can be widely employed in the forecasting field [35]. Moreover, the SVM has better performance in terms of electricity load forecasting [50–52]. According to Vapnik's theory, SVM equations are mainly expressed as follows.

Suppose p_i means the input vector, $p_i \in R^n$, and z_i implies the output vector, $z_i \in R$. The estimation expression is represented as:

$$f(p) =< w, \tau(p) > +q \tag{10}$$

where $\tau(p)$ is nonlinear mapping that causes the input space p to be high-dimensional space,

w denotes the estimated weight vectors, and q represents a scalar. The values of w and q can be obtained by means of a quadratic programming problem:

$$\begin{aligned} &\min_{\omega,q,\eta} \frac{1}{2} \parallel w^2 \parallel + C\sum_{i=1}^{N} (\eta_i + \eta_i^*) \\ &s.t. \begin{cases} |z_i - < w, \tau(p_i) > -q| \leq \varepsilon + \eta_i \\ \eta_i, \eta_i^* \geq 0, i = 1, 2, \ldots, N \end{cases} \end{aligned} \tag{11}$$

where C is the error penalty coefficient, N is the quantity of factors in the training sequence of training, η_i and η_i^* are the relaxation factor, and ε represents the admissible error. For nonlinear regression cases, we can convert them into linear regression cases using a kernel function $k(p_i, p_j)$. The nonlinear mapping can be obtained by:

$$f(p) = \sum_{i=1}^{N} (\sigma_i - \sigma_i^*) k(p, p_i) + q \tag{12}$$

where σ_i and σ_i^* are the Lagrange multipliers. The RBF kernel function is used in this paper, and can be written as follows:

$$k(p_i, p_j) = \exp(-\gamma \| p_i - p_j \|^2) \tag{13}$$

where γ denotes the kernel parameter, and p_i and p_j are two vectors in the input space. In this paper, two important parameters (γ, C) influence the prediction validity. The MFO algorithm is employed to determine the parameters.

Moth-Flame Optimization (MFO)

Mirjalili [53] provided a new metaheuristic algorithm known as MFO, a nature-inspired optimization method, by modeling the natural behavior of moths in a mathematical form. A specific presentation of this optimization method can be found in [53,54], and the main procedures are presented as follows.

Step 1 Parameter determination.

The parameters of the MFO method mainly include the quantity of moths, flames, and variables, the maximum number of iterations, and the lower and upper bounds of variables.

Step 2 Position initialization.

Equations (14) and (15) are introduced to express the position of moths and flames separately:

$$\boldsymbol{U} = \begin{bmatrix} u_{1,1} & u_{1,2} & \cdots & u_{1,d} \\ u_{2,1} & u_{2,2} & \cdots & u_{2,d} \\ \vdots & \vdots & \vdots & \vdots \\ u_{k,1} & u_{k,2} & \cdots & u_{k,d} \end{bmatrix} \tag{14}$$

$$\boldsymbol{V} = \begin{bmatrix} V_{1,1} & V_{1,2} & \cdots & V_{1,d} \\ V_{2,1} & V_{2,2} & \cdots & V_{2,d} \\ \vdots & \vdots & \vdots & \vdots \\ V_{k,1} & V_{k,2} & \cdots & V_{k,d} \end{bmatrix} \tag{15}$$

where k represents the quantity of moths, and d is the quantity of variables.

Equation (16) calculates the initialization of $\boldsymbol{U}$ and $\boldsymbol{V}$:

$$u_{\cdot h} \ \boldsymbol{or} \ V_{\cdot h} = (Ub_h - Lb_h) \times rand(\,) + Lb_h \tag{16}$$

where $u_{\cdot h}$ and $V_{\cdot h}$ denote the values of U and V separately, the upper and lower bounds of variables are represented by Ub and Lb, respectively, and $rand$ is a random number in [0, 1].

Step 3 Selection of fitness values.

For the flames, there is a matrix $\boldsymbol{OV}$, as shown in Equation (17), which can be used to obtain the corresponding fitness values:

$$\boldsymbol{OV} = \begin{bmatrix} OV_1 \\ OV_2 \\ \vdots \\ OV_k \end{bmatrix} \quad (17)$$

where k implies the moths' number.

Step 4 Iteration optimization.

A logarithmic spiral is selected as the update formula for the MFO method, as follows:

$$U_c = S(U_c, V_h) = G_c \cdot e^{br} \cdot cos(2\pi r) + V_h \quad (18)$$

G_c can be determined by:

$$G_c = |V_h - U_c| \quad (19)$$

where G_c represents the distance between the h-th flame and c-th moth, S implies the spiral function, b is equivalent to a constant for determining the logarithmic spiral form, and the value of r is randomly within the range of $[-1, 1]$. Moreover, the parameter r indicates how close the next position is to the flame; when the position is farthest, $r = 1$, while $r = -1$ implies the closest.

However, the method of updating the position defined by Equation (18) causes the MFO algorithm to converge to the local optimal solution quickly. To avoid converging to local optima, every moth can only refresh its location based on one of the flames, following Equation (18). The flames are sorted according to fitness values for each iteration and at the back of renovation. Next, the moths renew their corresponding flame locations; however, the location renovating of moths of approximately k various positions impairs the exploitation of optimal solutions. An adaptive mechanism is therefore proposed to address this problem:

$$flame\ no = round\left(W - s \times \frac{W-1}{iter_{\max}}\right) \quad (20)$$

where W implies the maximum quantity of flames, s indicates the number of current iterations, and $iter_{\max}$ is the maximum number of iterations.

Step 5 Optimal flames selection.

If the flame is not determined to be superior to the optimal flame of the former iteration, the flame's position will be updated, and the most appropriate flame is re-decided. When the iteration standard is reached, the optima are regarded as the most suitable approximation of the optimum. The pseudo-code of MFO is described in Algorithm 1:

Algorithm 1 Moth-Flame Optimization Algorithm.

***Input*:**

$T_a = (T(1), T(2), \ldots, T(s))$ —a series of training data

$T_b = (T(s+1), T(s+2), \ldots, T(s+t))$ —a series of verifying data

***Output*:**

x_{best} —the value which meet the best fitness in the back of global searching

***Parameters*:**

k—the quantity of moths and flames

d—the quantity of variables

$iter_{\max}$ —the maximum number of iterations

F_c —the fitness of moth *c*

s—the current iteration number

Ub/*Lb*—the upper/lower bound of variables

/* Determine the parameters of MFO. */
/* Initialize the moth $\boldsymbol{U}_c (c = 1, 2, \ldots, k)$ in random positions. */
FOR EACH $c = 1:k$ **DO**
  Calculate the corresponding fitness value F_c
END FOR
WHILE ($s \leq iter_{\max}$) **DO**
  /* Replace the position of $\boldsymbol{U}_c$ */
  $flame\ no = round(W - s * (W - 1)/iter_{max})$
  Evaluate the corresponding fitness function F_c
  IF ($s == 1$**) THEN**
    The moths are sorted: $\boldsymbol{V}$ = sort($\boldsymbol{U}$), $\boldsymbol{OV}$ = sort($\boldsymbol{OU}$)
  ELSE
    The moths are sorted: $\boldsymbol{V}$ = sort ($\boldsymbol{U}_{t-1}$, $\boldsymbol{U}_t$), $\boldsymbol{OV}$ = sort ($\boldsymbol{U}_{t-1}$, $\boldsymbol{U}_t$)
  END IF
  FOR EACH $c = 1:k$ **DO**
    FOR EACH $h = 1:d$ **DO**
      /* Update *r* */
      Determine *G* with respect to the moth $G_c = |V_h - U_c|$
      /* Update $U(c,h)$ in relation to the matching moth */
      $U_c = S(U_c, V_h)$, $S(U_c, V_h) = G_c \cdot e^{br} \cdot cos(2\pi r) + V_h$
    END FOR
  END FOR
END WHILE
RETURN x_{best}

Construction of the Final Forecasting Result

The construction of final forecasting result is the important step in the combined forecasting model. To overcome the above-mentioned drawbacks of linear combined model, the modified support vector machine based on MFO algorithm is developed in this paper, which is employed as a nonlinear combined method to search for the best function to combine each individual predictor. More specifically, the obtained function is performed to aggregate all forecasting results of each predictor in the previous steps as a final forecasting result for the original electric power load data. In other words, based on the previous work, the forecasting results obtained from each individual predictor are input into the modified SVM model to predict future electrical load data, which can achieve desirable forecasting performance in engineering applications.

3.3. Module 3: Evaluation

It is vital to evaluate the forecasting system's performance by employing appropriate metrics. To evaluate the forecasting accuracy, several evaluation criteria are applied in this study, including average error (AE), mean absolute error (MAE), mean square error (MSE), mean absolute percentage error (MAPE) and ζ_{INDEX}. Furthermore, for further verification of the model's effectiveness and significance, the Diebold-Mariano (DM) test and forecasting effectiveness are performed in this work.

3.3.1. Forecasting System Evaluation Criteria

Several evaluation criteria are applied in this study, as shown in Table 1, where O_i is the observed value, $\hat{F}_i$ means the predictive value and T represents the number of prediction values. In addition, the metric ζ_{INDEX} is employed to compare the forecasting effectiveness of the proposed combined model with other models.

Table 1. Evaluation rules.

Metric	Definition	Equation
AE	The average error of T forecasting results	$\frac{1}{T}\sum_{i=1}^{T}(O_i-\hat{F}_i)$
MAE	The mean error absolute of T forecasting results	$\frac{1}{T}\sum_{i=1}^{T}\lvert O_i-\hat{F}_i\rvert$
MSE	The mean square error of T forecasting results	$\frac{1}{T}\sum_{i=1}^{T}(O_i-\hat{F}_i)^2$
MAPE (%)	The mean absolute percentage error	$\frac{1}{T}\sum_{i=1}^{T}\left\lvert\frac{(O_i-\hat{F}_i)}{O_i}\right\rvert\times 100\%$
ζ_{INDEX} [1] (%)	The decreased relative error of the index among different models	$\frac{INDEX_{\text{model}_i}-INDEX_{\text{model}_j}}{INDEX_{\text{model}_i}}\times 100\%$

[1] In this paper, the *INDEX* includes MAE, MSE, MAPE.

3.3.2. DM Test

The DM test [55] is applied in order to contradistinguish the predictive validity of the proposed forecasting system from others. The details are as follows:

Assume that the real values are $\{y_t; t=1,\ldots,n+m\}$, and the predictions of the compared models are, respectively: $\{\hat{y}_t^{(a)}; t=1,\ldots,n+m\}$ $\{\hat{y}_t^{(b)}; t=1,\ldots,n+m\}$. Then, the prediction errors of these two models are:

$$e_{n+l}^{(a)} = y_{n+l} - \hat{y}_{n+l}^{(a)}, \quad l=1,2,\ldots,m. \tag{21}$$

$$e_{n+l}^{(b)} = y_{n+l} - \hat{y}_{n+l}^{(b)}, \quad l=1,2,\ldots,m. \tag{22}$$

The loss function $F(e_{n+g}^{(j)})$ $j=a,b$ is used for evaluating the forecasting accuracy of the compared models. Two popular loss functions reveal the following:

Square error loss:

$$F\left(e_{n+l}^{(j)}\right) = \left(e_{n+l}^{(j)}\right)^2 \tag{23}$$

Absolute deviation loss:

$$F\left(e_{n+l}^{(j)}\right) = \left|e_{n+l}^{(j)}\right| \tag{24}$$

The DM test statistic values are defined as:

$$DM = \frac{\sum_{l=1}^{m}\left(F\left(e_{n+l}^{(a)}\right) - F\left(e_{n+l}^{(b)}\right)\right)/m}{\sqrt{S^2/m}} s^2 \tag{25}$$

where S^2 is a variance estimator of $d_l = F(e_{n+l}^{(a)}) - F(e_{n+l}^{(b)})$. The hypothesis testing is:

$$H_0 : E(d_l) = 0 \; \forall t \tag{26}$$

$$H_1 : E(d_l) \neq 0 \tag{27}$$

The test statistics of DM gradually follow a standardized normal distribution. When the value of DM satisfies a criterion, which is represented by Equation (28), the null hypothesis will be refused:

$$|DM| > z_{\alpha/2} \tag{28}$$

where $z_{\alpha/2}$ expresses the z-value from the standardized normal table and the level of significance is α.

3.3.3. Forecasting Effectiveness

This work also introduces the forecasting effectiveness to measure the prediction veracity of the proposed forecasting system. Further details regarding forecasting effectiveness can be found in [56].

Definition 5. *Assume that the actual values are* $\{B_m; m = 1, \ldots, M\}$*, forecast values are* $\{\hat{B}_m; m = 1, \ldots, M\}$*, and forecast errors are* $e_m = B_m - \hat{B}_m$*. Then, the forecasting accuracy is calculated by:*

$$A_m = \begin{cases} 1 - \left|\frac{e_m}{B_m}\right|, 0 \leq \left|\frac{e_m}{B_m}\right| \leq 1 \\ 0, \left|\frac{e_m}{B_m}\right| > 1 \end{cases} \tag{29}$$

Definition 6. *The kth-order forecasting effectiveness unit can be calculated as:*

$$n^k = \sum_{m=1}^{M} Q_m A_m^k \tag{30}$$

where k represents a positive integer, Q_m *expresses the discontinuous probability distribution at time m, and* $\sum_{m=1}^{M} Q_m = 1, Q_m > 0$*. Moreover, when the priori information of the discrete probability distribution cannot be known, we define* Q_m *as equal to* $1/M$*.*

Definition 7. *The kth-order forecasting effectiveness can be represented as:*

$$E\left(n^1, n^2, \cdots, n^k\right) \tag{31}$$

where E indicates a continuous function of a certain k unit. In particular, when $E(x) = x$*, the formula for one-order forecasting effectiveness can be expressed as* $E(n^1) = n^1$*; when* $E(x, y) = x\left(1 - \sqrt{y - x^2}\right)$*, the formula for two-order forecasting effectiveness can be expressed as* $E(n^1, n^2) = n^1(1 - \sqrt{n^2 - (n^1)^2})$*.*

4. Experimental Study

All experiments are conducted in MATLAB R2015a on Windows 10 with a 2.60 GHz Intel Core i7-6700HQ CPU, 64-bit and 8 GB RAM. The experimental parameters are displayed in Table 2.

Table 2. Experimental parameter values.

Model	Experimental Parameter	Default Value
CEEMDAN	Noise standard deviation	0.2
	The number of realizations	500
	Maximum number of sifting iterations	5000
	The removed intrinsic mode functions	IMF1
BPNN	Learning velocity	0.1
	Maximum number of training iterations	1000
	Training precision requirement	0.00004
	Neuron number in the input layer	4
	Neuron number in the hidden layer	9
	Neuron number in the output layer	1
FABPNN	FA number of fireflies	30
	Maximum number of FA iterations	500
	FA randomness 0–1	0.5
	FA minimum value of beta	0.2
	FA absorption coefficient	1
	BPNN maximum number of iteration times	200
	BPNN convergence value	0.00001
	BPNN learning rate	0.1
	Neuron number in the input layer	4
	Neuron number in the hidden layer	9
	Neuron number in the output layer	1
ENN	Number of iterations	1000
	Neuron number in the input layer	4
	Neuron number in the hidden layer	9
	Neuron number in the output layer	1
WNN	Number of iterations	100
	Learning rate	0.01
	Neuron number in the input layer	4
	Neuron number in the hidden layer	9
	Neuron number in the output layer	1
MFO	The number of search agents	30
	Maximum number of iterations	300
	The lower bounds of variables	0.01
	The upper bounds of variables	100
	The number of variables	2
SVM	The number of the input layer	4
	The number of the output layer	1
	The kernel function's name	RBF

4.1. Data Selection

In this study, half an hour of power load data from New South Wales in February and June from 2009 to 2011 are selected to assess the validity of the proposed combined forecasting system, as indicated in Table 3. To enhance the forecasting performance, a longitudinal data selection is accepted to preprocessing the raw data. Each series of raw load datasets is divided into seven subclasses (from Monday to Sunday), based on a designated date of one week, to ensure that the inherent characteristics of each subset are the same. Figure 3 demonstrates the longitudinal data selection process. For instance, there are 12 Mondays (48 data points per day) in February from 2009 to

2011, which are selected as one subset. For each subset, we select the last one day as the testing set and the other days as the training set. The training and testing data structures of the proposed combined forecasting system are illustrated in Figure 1 part II.

Table 3. Statistical values of data used in this study.

Week	Month	Mean (MW)	Median (MW)	Std. (MW)	Minimum (MW)	Maximum (MW)
MON.	February	9334.305	9871.095	1520.628	6649.840	11,078.940
	June	9720.624	9952.190	1409.115	7157.530	11,937.500
TUE.	February	8589.615	9019.185	1073.913	6488.980	9683.760
	June	9920.198	10,129.775	1238.084	7453.350	11,996.360
WED.	February	8649.826	9031.205	1111.026	6452.950	9786.950
	June	9682.923	9848.785	1189.045	7228.830	11,713.400
THU.	February	8864.992	9374.700	1255.005	6487.110	10,273.970
	June	9603.785	9743.965	1206.705	7140.740	11,602.130
FRI.	February	8870.044	9170.695	1237.710	6516.410	10,200.400
	June	9735.629	9894.510	1182.482	7327.950	11,451.680
SAT.	February	8540.942	8979.640	1133.162	6554.520	9928.520
	June	9124.386	9226.755	982.705	7268.430	10,864.100
SUN.	February	8093.038	8554.020	1001.747	6391.530	9390.940
	June	8772.331	8663.305	1116.673	6977.150	10,926.030

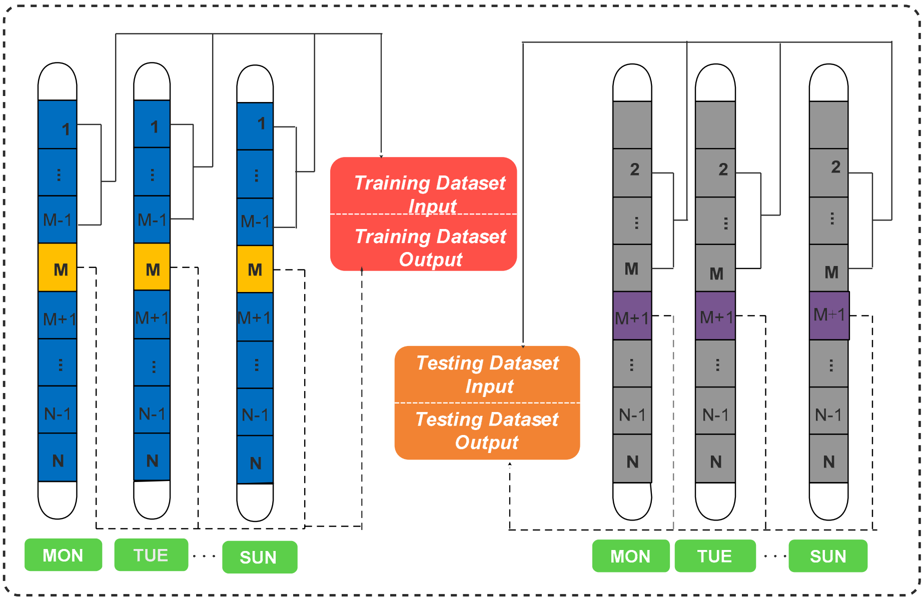

Figure 3. Process of longitudinal data selection.

4.2. Experiment Setup

To test the performance of the developed nonlinear combined forecasting system, three experiments are conducted in this study. The electrical load data collected from New South Wales in February from 2009 to 2011 are used as Experiment I in this study. Meanwhile, due to the different electrical load datasets with different characteristics, the datasets of June are also used as another case study, called Experiment II, which is employed to further test the forecasting superiority of the proposed combined forecasting system. In Experiment I-II, the developed combined forecasting system is compared with other individual forecasting models, namely, BPNN, FABPNN, ENN and WNN. If the proposed forecasting system performs better than other individual models in different months, we can safely conclude that the proposed system has better forecasting performance and universal applicability for different datasets with different characteristics; in other words, the proposed combined forecasting system based on improved data preprocessing and modified SVM can achieve better forecasting performance than other comparison models in different environments. Moreover, the benchmark model ARIMA was employed to evaluate and compare the developed combined forecasting system in Experiment III based on the electrical load data of February and June.

4.2.1. Experiment I: The Case of February

In this experiment, to test the forecasting performance of the novel nonlinear forecasting system by improved data preprocessing and modified SVM, the 30-min electrical data from Monday to Sunday in February are employed. More specifically, four performance metrics, significant improvements for combined model compared with the forecasting results of other models and statistical MAPE values are used to evaluate the foresting accuracy and stability of the proposed forecasting system. The multi-step prediction results of the developed combined forecasting system and single models are displayed in Tables 4–6, and Figures 4 and 5.

(a) Table 4 shows the prediction capability of the combined forecasting system and four single models in the 1-step to 3-step forecasting. Taking Fridays' forecasting results as an example: in 1-step forecasting, it is determined that the proposed nonlinear combined forecasting system achieves superior results compared to other models for different forecasting horizons. The combined forecasting system exhibits minimum forecasting errors, with AE, MAE, MSE, and MAPE values of −3.7850, 41.5131, 2979.40, and 0.4739%, respectively. The forecasting ability of BPNN is ranked second, while WNN exhibits the worst forecasting performance. In 2-step forecasting, the combined forecasting system achieves the most exact prediction performance, with a MAPE value of 0.8163%, while BPNN is the second most accurate model, and WNN is the worst. For 3-step forecasting, the combined forecasting system still achieves the most superior performance. The 1-step forecasting exhibits superior forecasting accuracy for the same model compared with multi-step prediction.

(b) Table 5 presents the detailed results of multi-step improvements between the developed combined forecasting system and other prediction models. Taking Fridays' results: in the 1-step predictions, the combined forecasting system decreases the MAE values by 57.4973%, 58.9966%, 61.2416% and 71.2267%, the MSE values by 82.4779%, 83.4804%, 84.4607% and 91.0522%, and the MAPE values by 57.6094%, 59.3157%, 61.7676% and 72.2005%, based on BPNN, FABPNN, ENN and WNN, respectively. In the 2-step and 3-step predictions, the combined forecasting system still decreases the MAE, MSE and MAPE values in comparison with other models.

(c) Table 6 shows the statistical values of MAPE (%). The developed combined forecasting system obtains lower minimum and maximum MAPE values among the four individual models for 1-step to 3-step prediction. Furthermore, the developed forecasting system achieves minimum standard deviation (Std.) values for MAPE compared to the individual models.

(d) Figure 4 displays the average values of AE, MAE, MSE and MAPE for 1-step, 2-step, and 3-step forecasting. To analyze the detailed forecasting results, the 1-step forecasting results for Monday are depicted in Figure 5. It can be observed that the prediction validity of the proposed nonlinear combined forecasting system is more precise than that of the single models. Moreover, the forecasting values of the developed forecasting system are more approximate to the real data.

Table 4. Forecasting results obtained using February data from New South Wales.

Week	Model	AE			MAE			MSE			MAPE		
		1-Step	2-Step	3-Step	1-Step	2-Step	3-Step	1-Step	2-Step	3-Step	1-Step	2-Step	3-Step
MON.	BPNN	1.3639	−10.7514	−14.7858	76.9680	87.3096	126.8697	9493.46	12,421.47	27,525.35	0.8632	0.9558	1.4429
	FABPNN	3.7445	−6.6519	−5.2474	76.7589	88.2479	128.2259	9547.03	12,511.88	28,258.78	0.8612	0.9670	1.4564
	ENN	−1.0044	−13.5185	−15.2619	84.9175	105.2535	152.5501	12,425.12	18,729.96	41,127.41	0.9535	1.1599	1.7416
	WNN	−0.1408	−25.7658	−26.4372	134.9493	174.9007	236.5244	32,121.24	66,146.46	183,341.01	1.5029	1.9178	2.6471
	Combined forecasting system	−1.8954	4.8475	−25.3053	42.7547	55.7483	92.0454	2955.29	5066.13	15,392.98	0.4896	0.6125	1.0435
TUE.	BPNN	−14.0677	−23.9245	−32.1850	82.8839	104.7622	135.1333	11,424.72	19,811.92	32,025.02	0.9856	1.2580	1.6543
	FABPNN	−16.8212	−28.3703	−39.8426	87.0675	111.3953	140.6762	12,832.80	22,262.70	34,626.02	1.0341	1.3385	1.7184
	ENN	−20.6985	−32.9486	−42.9214	104.1221	134.5153	158.6410	17,145.19	30,481.01	45,606.38	1.2659	1.6504	1.9700
	WNN	−18.6602	−31.9576	−50.3965	132.1093	179.5787	231.9993	32,314.95	95,482.40	228,634.12	1.6168	2.2088	2.8686
	Combined forecasting system	−3.5775	−3.1009	−1.3271	48.7534	72.6386	109.7521	3697.70	9420.42	21,857.92	0.5921	0.8679	1.3137
WED.	BPNN	−17.0143	−31.5453	−35.0435	79.8144	113.2511	144.3384	10,635.37	23,724.32	36,327.29	0.9491	1.3497	1.7504
	FABPNN	−15.8284	−30.8274	−33.7778	83.1057	113.8130	139.9802	11,747.10	24,310.67	34,389.39	0.9930	1.3608	1.6969
	ENN	−13.7888	−25.2383	−26.1058	87.7993	117.0281	142.4337	13,134.19	25,093.04	35,466.31	1.0498	1.3961	1.7187
	WNN	−11.8223	−12.5006	−3.6612	118.3172	160.6506	198.1202	41,894.21	58,325.44	79,324.94	1.4270	1.9408	2.3941
	Combined forecasting system	−8.1485	−9.1175	−28.6959	49.4339	68.0790	104.9988	4082.45	9029.29	21,231.04	0.5998	0.8124	1.2458
THU.	BPNN	−6.3561	−19.6933	−22.5452	104.6001	132.4169	174.4194	17,715.78	32,893.48	47,678.25	1.2009	1.5345	2.0338
	FABPNN	−8.0497	−22.9996	−23.4411	102.1040	129.9880	166.0143	17,458.21	32,981.15	43,922.02	1.1714	1.5080	1.9394
	ENN	−14.2674	−30.6256	−29.6502	114.5853	143.5429	171.5193	21,097.11	36,114.88	45,852.66	1.3363	1.6930	2.0229
	WNN	−33.6208	−53.1476	−63.9543	160.5429	200.8806	247.5782	45,415.21	82,931.44	124,086.68	1.8929	2.3803	2.9301
	Combined forecasting system	−6.5061	−10.1216	−4.2527	55.5226	80.3931	123.8744	4824.10	12,375.84	24,987.70	0.6553	0.9407	1.4463
FRI.	BPNN	−10.2567	−23.5966	−21.2707	97.6717	140.9842	187.9748	17,003.61	37,922.83	61,624.94	1.1179	1.6060	2.1836
	FABPNN	−14.0009	−28.2144	−28.2492	101.2430	147.2809	198.5211	18,035.56	41,018.75	69,155.70	1.1647	1.6898	2.3062
	ENN	−12.1384	−27.6435	−22.5750	107.1073	146.7995	190.7033	19,173.26	38,936.81	59,817.36	1.2394	1.7010	2.2384
	WNN	−28.1042	−47.9970	−52.1578	144.2766	196.5340	258.1345	33,297.40	66,162.33	108,392.63	1.7046	2.3169	3.0409
	Combined forecasting system	−3.7850	−0.8954	−3.4699	41.5131	71.7784	105.1659	2979.40	10,037.04	22,513.69	0.4739	0.8163	1.1747
SAT.	BPNN	−18.3668	−58.8065	−50.1905	83.6567	128.2100	149.5539	13,347.26	30,695.80	42,244.56	0.9949	1.5385	1.8127
	FABPNN	−18.2990	−58.7480	−52.0260	81.0710	122.2612	142.6670	12,678.25	27,997.98	37,079.79	0.9596	1.4585	1.7135
	ENN	−8.9057	−33.5612	−33.2007	88.3301	129.8825	159.4560	13,860.60	28,814.81	43,314.43	1.0473	1.5408	1.8951
	WNN	−76.2241	−103.5840	−110.5893	161.0754	203.1411	247.7138	107,836.75	137,768.64	166,982.05	1.9893	2.5032	3.0492
	Combined forecasting system	−9.9972	−15.8985	−16.9380	42.2213	60.0048	97.4307	3253.00	7601.39	16,427.04	0.5115	0.7260	1.1988
SUN.	BPNN	−19.0006	−41.8885	−63.0577	87.1693	138.3510	146.6729	11,695.38	30,279.09	41,649.76	1.0927	1.7384	1.8840
	FABPNN	−14.7801	−33.2463	−50.9624	87.4692	134.0810	144.3636	11,198.22	26,233.76	34,582.41	1.0840	1.6733	1.8233
	ENN	−14.2234	−29.7956	−42.5369	81.0386	123.0542	124.7987	10,251.81	22,741.01	23,536.69	1.0041	1.5374	1.5672
	WNN	−30.0213	−49.0184	−68.3288	113.8393	164.9003	194.3404	19,452.64	42,417.10	64,463.36	1.4473	2.1072	2.5010
	Combined forecasting system	−3.1120	3.1278	−17.6043	40.6275	55.6796	74.5055	2549.95	5992.00	10,360.29	0.4988	0.6746	0.9197

Table 5. Improvement percentages generated by the combined forecasting system from February data.

Week		Combined Forecasting System vs. BPNN			Combined Forecasting System vs. FABPNN			Combined Forecasting System vs. ENN			Combined Forecasting System vs. WNN		
		1-Step	2-Step	3-Step	1-Step	2-Step	3-Step	1-Step	2-Step	3-Step	1-Step	2-Step	3-Step
MON.	ζ_{MAE}	44.4513	36.1488	27.4489	44.2999	36.8276	28.2162	49.6514	47.0343	39.6622	68.3179	68.1258	61.0842
	ζ_{MSE}	68.8703	59.2147	44.0771	69.0449	59.5094	45.5285	76.2152	72.9517	62.5725	90.7996	92.3410	91.6042
	ζ_{MAPE}	43.2778	35.9101	27.6819	43.1419	36.6539	28.3536	48.6478	47.1907	40.0867	67.4188	68.0597	60.5802
TUE.	ζ_{MAE}	41.1787	30.6634	18.7823	44.0051	34.7921	21.9825	53.1767	45.9998	30.8173	63.0962	59.5506	52.6929
	ζ_{MSE}	67.6343	52.4507	31.7474	71.1856	57.6852	36.8743	78.4330	69.0941	52.0727	88.5573	90.1339	90.4398
	ζ_{MAPE}	39.9223	31.0096	20.5897	42.7370	35.1567	23.5513	53.2227	47.4119	33.3134	63.3761	60.7058	54.2041
WED.	ζ_{MAE}	38.0639	39.8867	27.2551	40.5168	40.1834	24.9902	43.6966	41.8268	26.2823	58.2192	57.6229	47.0025
	ζ_{MSE}	61.6144	61.9408	41.5562	65.2472	62.8587	38.2628	68.9174	64.0167	40.1375	90.2553	84.5191	73.2354
	ζ_{MAPE}	36.7974	39.8068	28.8274	39.5934	40.2975	26.5832	42.8602	41.8081	27.5157	57.9655	58.1405	47.9638
THU.	ζ_{MAE}	46.9192	39.2879	28.9790	45.6216	38.1534	25.3833	51.5448	43.9937	27.7782	65.4157	59.9797	49.9655
	ζ_{MSE}	72.7695	62.3760	47.5910	72.3678	62.4760	43.1089	77.1339	65.7320	45.5044	89.3778	85.0770	79.8627
	ζ_{MAPE}	45.4345	38.6991	28.8866	44.0607	37.6218	25.4225	50.9610	44.4366	28.5023	65.3818	60.4796	50.6387
FRI.	ζ_{MAE}	57.4973	49.0877	44.0532	58.9966	51.2643	47.0253	61.2416	51.1045	44.8537	71.2267	63.4779	59.2593
	ζ_{MSE}	82.4779	73.5330	63.4666	83.4804	75.5306	67.4449	84.4607	74.2222	62.3626	91.0522	84.8297	79.2295
	ζ_{MAPE}	57.6094	49.1712	46.2056	59.3157	51.6906	49.0637	61.7676	52.0078	47.5228	72.2005	64.7666	61.3709
SAT.	ζ_{MAE}	49.5303	53.1980	34.8525	47.9206	50.9208	31.7076	52.2005	53.8007	38.8981	73.7879	70.4615	60.6680
	ζ_{MSE}	75.6279	75.2364	61.1144	74.3419	72.8502	55.6981	76.5306	73.6199	62.0749	96.9834	94.4825	90.1624
	ζ_{MAPE}	48.5887	52.8144	33.8674	46.6971	50.2268	30.0376	51.1612	52.8833	36.7424	74.2879	70.9991	60.6855
SUN.	ζ_{MAE}	53.3925	59.7548	49.2029	53.5523	58.4732	48.3903	49.8665	54.7520	40.2994	64.3116	66.2344	61.6624
	ζ_{MSE}	78.1970	80.2108	75.1252	77.2290	77.1592	70.0417	75.1268	73.6511	55.9824	86.8915	85.8736	83.9284
	ζ_{MAPE}	54.3518	61.1941	51.1820	53.9817	59.6848	49.5571	50.3214	56.1203	41.3132	65.5337	67.9861	63.2263

Table 6. Statistical MAPE values of February data from New South Wales.

Week		BPNN			FABPNN			ENN			WNN			Combined Forecasting System		
		1-Step	**2-Step**	**3-Step**	**1-Step**	**2-Step**	**3-Step**	**1-Step**	**2-Step**	**3-Step**	**1-Step**	**2-Step**	**3-Step**	**1-Step**	**2-Step**	**3-Step**
MON.	**Minimum**	0.8263	0.8868	1.2521	0.8120	0.8529	1.1331	0.8120	0.9274	1.2315	0.9705	1.1373	1.3787	0.4529	0.5472	0.8730
	Maximum	0.9434	1.1193	1.7437	0.9823	1.2637	2.1828	1.0879	1.4398	2.1751	3.0041	4.0754	7.2584	0.5151	0.6505	1.2038
	Mean	0.8632	0.9558	1.4429	0.8612	0.9670	1.4564	0.9535	1.1599	1.7416	1.5029	1.9178	2.6471	0.4896	0.6125	1.0435
	Std.	0.0345	0.0657	0.1616	0.0487	0.1037	0.2740	0.0741	0.1385	0.2470	0.6015	0.9387	1.5568	0.0153	0.0289	0.0867
TUE.	**Minimum**	0.8513	1.0494	1.3943	0.8942	1.1293	1.4114	0.9588	1.2102	1.4313	1.0894	1.3884	1.7998	0.5608	0.7945	1.0911
	Maximum	1.1912	1.5185	1.9739	1.4806	1.8611	2.0036	1.5263	1.9735	2.3895	3.3843	6.9578	10.6987	0.6185	0.9187	1.5951
	Mean	0.9856	1.2580	1.6543	1.0341	1.3385	1.7184	1.2659	1.6504	1.9700	1.6168	2.2088	2.8686	0.5921	0.8679	1.3137
	Std.	0.0877	0.1299	0.1802	0.1493	0.2029	0.1622	0.1536	0.1937	0.2241	0.5693	1.3644	2.2010	0.0179	0.0366	0.1462
WED.	**Minimum**	0.8988	1.1342	1.3668	0.8959	1.0632	1.2543	0.9589	1.1811	1.3829	1.0015	1.2242	1.4547	0.5303	0.7643	0.7724
	Maximum	1.0376	1.4876	2.0036	1.3294	1.9717	2.3057	1.1692	1.5723	2.0403	3.2969	4.7078	4.4628	1.0370	0.8529	1.4643
	Mean	0.9491	1.3497	1.7504	0.9930	1.3608	1.6969	1.0498	1.3961	1.7187	1.4270	1.9408	2.3941	0.5998	0.8124	1.2458
	Std.	0.0376	0.0944	0.1750	0.1175	0.2126	0.2517	0.0692	0.1186	0.1846	0.5523	0.8268	0.6952	0.1223	0.0309	0.1919
THU.	**Minimum**	1.1328	1.3555	1.7345	1.0592	1.2446	1.6240	1.1695	1.4815	1.7197	1.4439	1.6901	1.9451	0.5996	0.6861	1.2255
	Maximum	1.6897	2.2229	3.1837	1.4571	2.0609	2.5822	1.4567	1.9075	2.4223	3.3581	5.0644	5.9695	0.6986	0.9970	1.7947
	Mean	1.2009	1.5345	2.0338	1.1714	1.5080	1.9394	1.3363	1.6930	2.0229	1.8929	2.3803	2.9301	0.6553	0.9407	1.4463
	Std.	0.1370	0.2010	0.3381	0.1043	0.1875	0.2672	0.0795	0.1300	0.2029	0.4819	0.8472	1.0381	0.0273	0.0761	0.1614
FRI.	**Minimum**	0.9789	1.3521	1.8090	0.9879	1.3789	1.9802	1.1533	1.5778	2.0425	1.1984	1.6895	2.1985	0.4217	0.7267	0.9891
	Maximum	1.3273	1.8529	2.6347	1.6243	2.1960	2.8817	1.5201	1.8915	2.4986	2.3440	3.0883	4.2423	0.5172	0.9259	1.4602
	Mean	1.1179	1.6060	2.1836	1.1647	1.6898	2.3062	1.2394	1.7010	2.2384	1.7046	2.3169	3.0409	0.4739	0.8163	1.1747
	Std.	0.0869	0.1481	0.2171	0.1625	0.2330	0.2601	0.0967	0.1050	0.1391	0.3505	0.4306	0.6477	0.0272	0.0508	0.1357
SAT.	**Minimum**	0.8925	1.4090	1.5762	0.8792	1.3074	1.5122	0.9497	1.4249	1.6132	0.9158	1.1241	1.3579	0.4807	0.6395	1.0126
	Maximum	1.0930	1.6887	2.1120	1.0835	1.6422	1.9560	1.2232	1.6595	2.1832	10.3437	11.1349	11.0434	0.5409	0.8148	1.4727
	Mean	0.9949	1.5385	1.8127	0.9596	1.4585	1.7135	1.0473	1.5408	1.8951	1.9893	2.5032	3.0492	0.5115	0.7260	1.1988
	Std.	0.0536	0.0912	0.1550	0.0573	0.0958	0.1237	0.0965	0.0795	0.1722	2.3444	2.4300	2.3140	0.0145	0.0472	0.1428
SUN.	**Minimum**	0.9423	1.4501	1.4459	0.9174	1.3993	1.4387	0.9367	1.4470	1.4025	1.0703	1.6719	1.6650	0.4750	0.4991	0.7836
	Maximum	1.7058	2.7597	3.6231	1.4369	1.9129	2.2679	1.1217	1.6749	1.8943	1.8294	2.6436	3.1335	0.5144	0.7494	1.0195
	Mean	1.0927	1.7384	1.8840	1.0840	1.6733	1.8233	1.0041	1.5374	1.5672	1.4473	2.1072	2.5010	0.4988	0.6746	0.9197
	Std.	0.2429	0.4149	0.6700	0.1215	0.1744	0.2622	0.0597	0.0552	0.1404	0.2072	0.2701	0.4509	0.0122	0.0784	0.0729

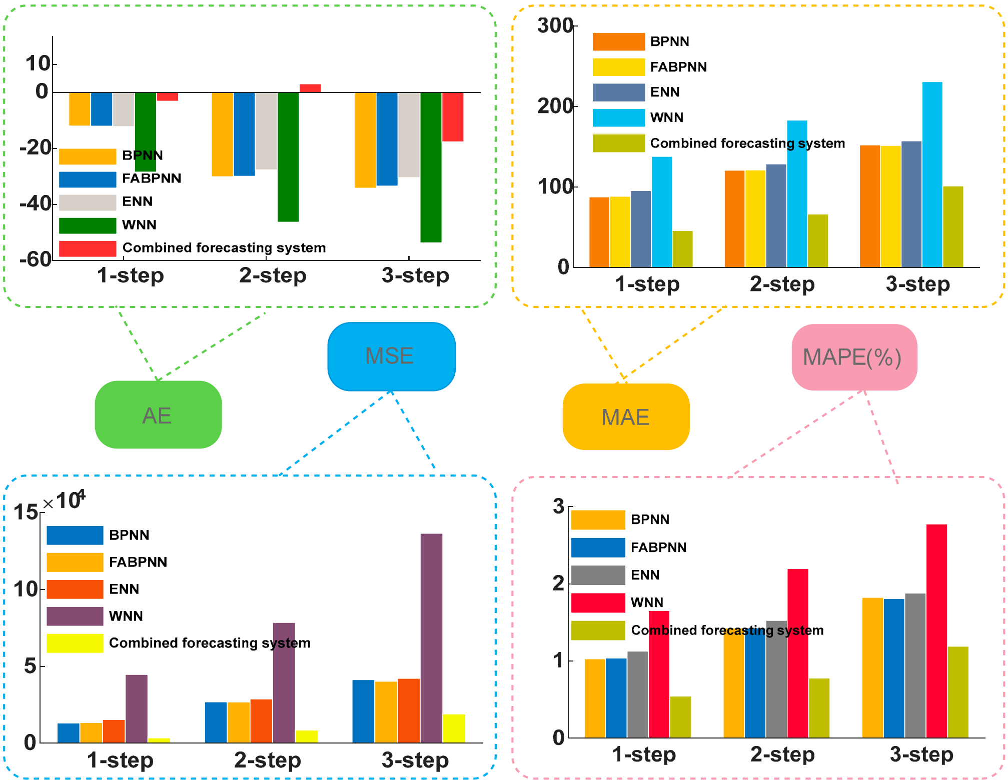

Figure 4. The results of AE, MAE, MSE and MAPE for February.

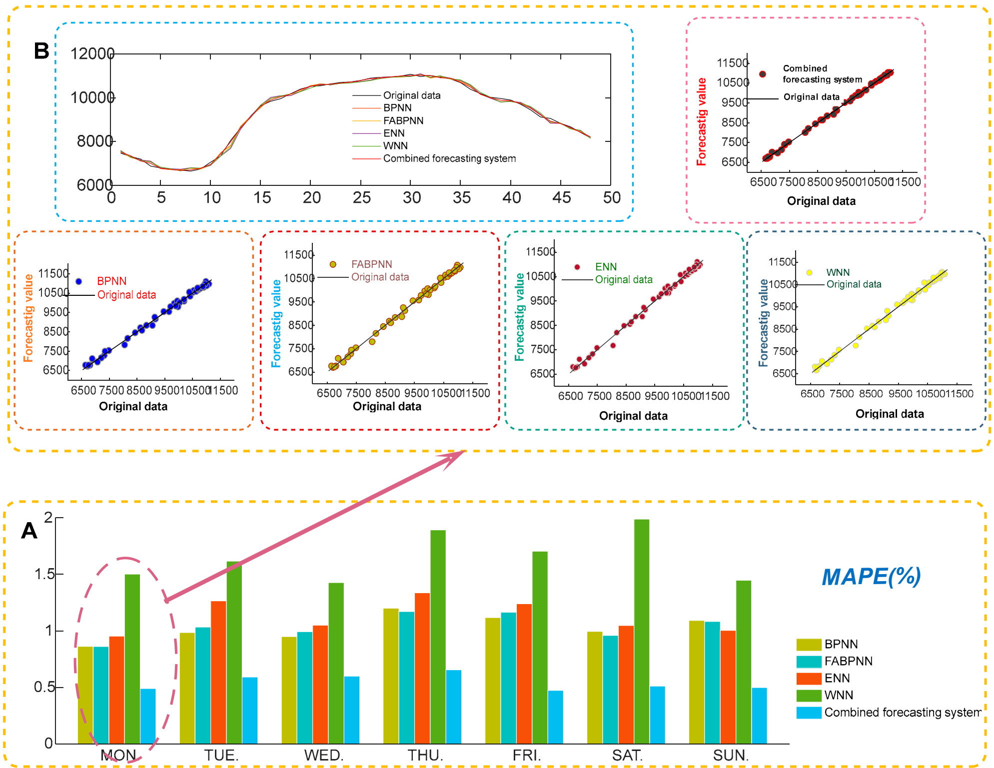

Figure 5. 1-step forecasting results in February. (**A**) The MAPE values from Monday to Sunday. (**B**) The forecasting results of Monday, February.

Remark. *By comparing the forecasting error metrics for multi-step prediction, it is found that the proposed forecasting system is superior in almost every aspect. Meanwhile, the developed combined forecasting system achieves the lowest minimum and maximum MAPE values, implying that it is more exact than the single models. The proposed combined forecasting system is the steadiest, because it achieves the minimum Std. values for MAPE. Therefore, the proposed forecasting system has better forecasting accuracy and high forecasting stability than the other models. Most importantly, the improved data preprocessing algorithm and modified SVM can act as an effective technique to improve the forecasting performance of the proposed system, which can effectively predict the electrical load data.*

4.2.2. Experiment II: The Case of June

To evaluate the forecasting performance of the developed combined forecasting system for different load datasets, the 30-min electrical data from Monday to Sunday in June are employed in Experiment II. The dataset structure is the same as that of February, and the results are displayed in Tables 7–9, and Figures 6 and 7.

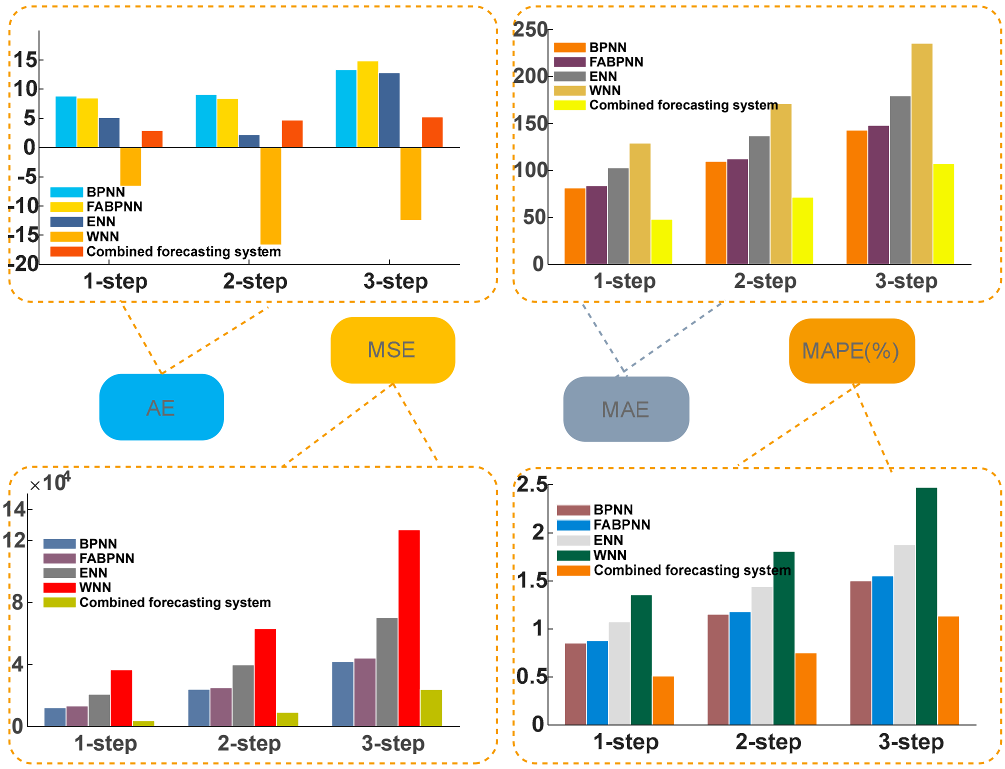

Figure 6. The results of AE, MAE, MSE and MAPE for June.

(a) Table 7 shows the final evaluations of the results for the 1-step to 3-step forecasting. For 1-step forecasting, the proposed combined forecasting system outperforms the BPNN, FABPNN, ENN and WNN models, according to the comparison of AE, MAE, MSE and MAPE from Monday to Sunday. For example, the MAPE values of the combined forecasting system are 0.5270%, 0.5390%, 0.4489%, 0.5306%, 0.4429%, 0.5052% and 0.5332% from Monday to Sunday, respectively. For 2-step forecasting, the developed combined forecasting system achieves the most accurate prediction effect, with MAPE values of 0.8562%, 0.7543%, 0.7336%, 0.8335%, 0.6223%, 0.6898% and 0.7702% from Monday to Sunday, respectively. For 3-step forecasting, the developed nonlinear combined forecasting system is still the most accurate.

(b) Table 8 illustrates the detailed multi-step improvements between the developed combined forecasting system and other prediction models. Taking the results of Sunday as an example, in the

1-step predictions, the combined forecasting system decreases the MAPE values by 49.1983%, 47.7906%, 59.3493% and 65.0099%, based on BPNN, FABPNN, ENN and WNN, respectively. In the 2-step and 3-step predictions, the proposed combined forecasting system also decreases the MAPE values.

(c) Table 9 displays the results of the MAPE value statistics. For the minimum, maximum, mean and Std. of the MAPE values, the developed combined forecasting system obtains a lower value in all aspects for BPNN, FABPNN, ENN and WNN.

(d) Figure 6 summarizes the results of the average values of four forecasting error indexes for 1-step, 2-step, and 3-step forecasting in June. Furthermore, Figure 7 illustrates the detailed forecasting results of 1-step for Sunday. It is found that the combined forecasting system achieves a more precise prediction performance than the other four models.

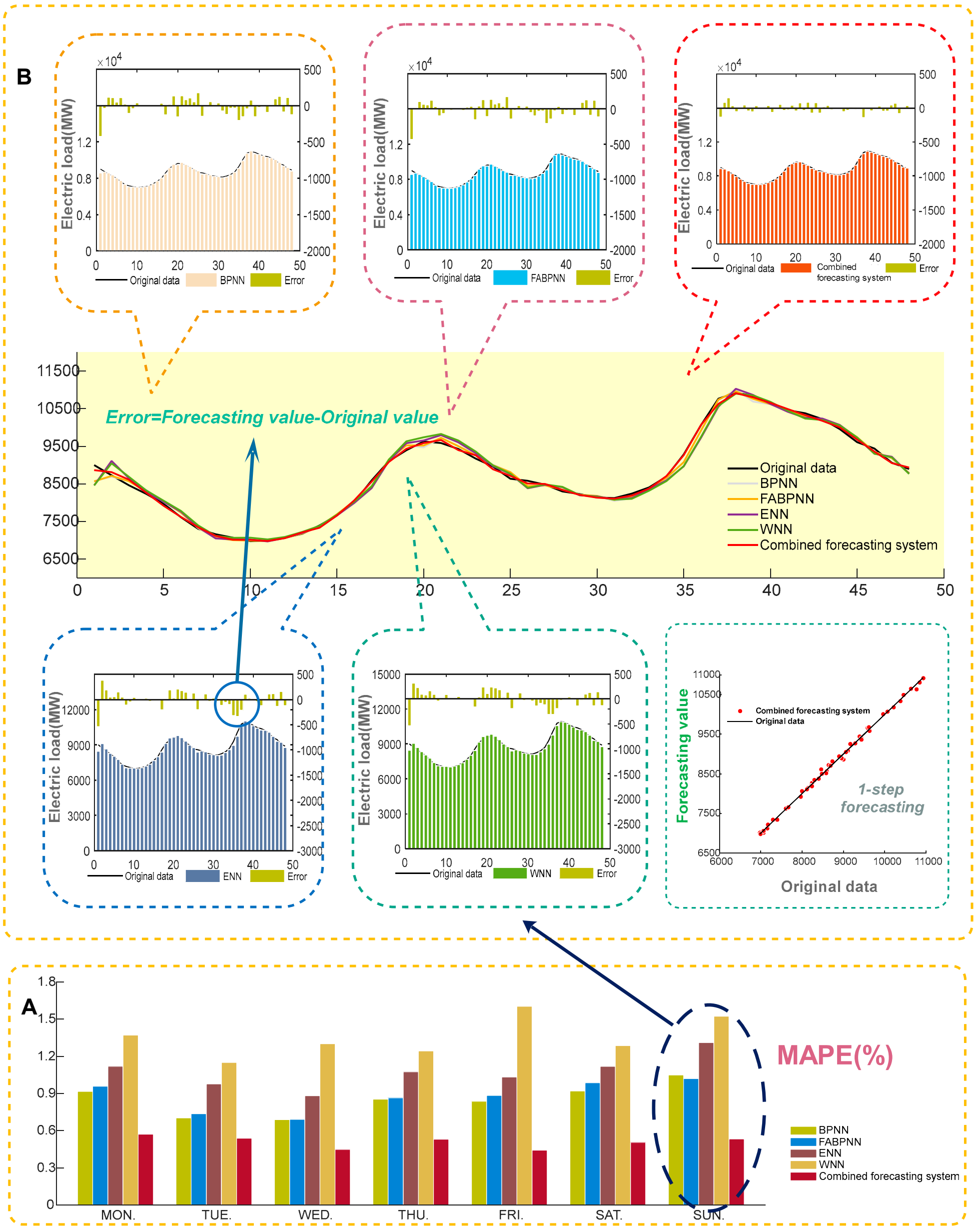

Figure 7. 1-step forecasting results in June. (**A**) The MAPE values from Monday to Sunday. (**B**) The forecasting results of Sunday, June

Table 7. Forecasting results obtained using June data from New South Wales.

Week	Model	AE			MAE			MSE			MAPE		
		1-Step	2-Step	3-Step	1-Step	2-Step	3-Step	1-Step	2-Step	3-Step	1-Step	2-Step	3-Step
MON.	BPNN	28.1490	40.2809	60.0420	87.2188	116.6938	157.3218	12,598.62	24,248.91	46,240.92	0.9174	1.2500	1.6564
	FABPNN	31.9426	43.4337	70.0051	91.8725	122.9630	174.0908	14,715.99	27,952.61	57,357.07	0.9592	1.3000	1.8176
	ENN	23.5497	25.6296	41.8058	107.7753	140.2308	191.1443	22,021.50	43,213.06	84,770.04	1.1190	1.4900	2.0180
	WNN	21.3635	24.2720	40.4258	131.7077	172.9343	259.7937	34,847.82	61,929.17	162,633.65	1.3722	1.8200	2.6891
	Combined forecasting system	13.1643	31.7783	33.2478	53.4406	81.4294	118.3925	4923.01	10,866.11	29,343.95	0.5720	0.8562	1.2510
TUE.	BPNN	11.8632	11.0946	30.6152	68.8202	93.5565	118.4368	7209.00	14,736.01	27,030.99	0.7028	0.9400	1.1964
	FABPNN	8.2711	4.7844	23.4885	72.6215	96.1279	127.4886	8652.02	16,947.82	31,041.00	0.7372	0.9600	1.2870
	ENN	9.9318	2.2467	25.5482	97.0374	117.4459	147.8419	16,480.67	30,382.58	52,207.81	0.9774	1.1800	1.4659
	WNN	8.3753	4.2323	24.5869	113.9295	142.2588	203.1351	22,966.51	40,516.86	91,325.84	1.1504	1.4300	2.0418
	Combined forecasting system	5.5324	5.2540	−0.8695	52.5606	74.6922	104.1388	4625.96	8844.65	20,139.94	0.5390	0.7543	1.0397
WED.	BPNN	−12.3035	−26.7509	−41.0592	67.7807	94.4602	135.4084	8288.43	17,216.81	34,143.77	0.6894	0.9568	1.3600
	FABPNN	−8.0366	−20.7559	−26.5353	67.4427	94.1133	136.7037	8505.36	17,816.29	36,375.57	0.6917	0.9612	1.3900
	ENN	−12.0552	−29.6080	−34.3218	86.6654	124.5985	175.2954	14,665.42	31,819.07	64,573.05	0.8824	1.2715	1.7700
	WNN	−42.7244	−70.8510	−97.8009	126.2426	167.1746	243.5229	38,007.57	60,350.02	123,256.04	1.3027	1.7200	2.4900
	Combined forecasting system	−4.8054	−10.0858	−26.1299	43.0172	70.9730	93.2434	2939.59	9012.51	16,351.51	0.4489	0.7336	0.9664
THU.	BPNN	−5.8352	−18.9423	−40.7135	82.8959	112.6687	151.2279	11,293.16	23,270.95	43,996.53	0.8543	1.1660	1.5612
	FABPNN	−9.7177	−24.0847	−54.5332	84.0990	111.3262	155.7279	11,357.10	21,913.86	44,006.92	0.8646	1.1457	1.6058
	ENN	−14.1086	−34.7318	−62.7759	104.5977	137.7137	201.8255	19,136.63	38,040.77	76,066.67	1.0751	1.4307	2.0714
	WNN	−27.2461	−54.1089	−91.1277	119.6625	160.5898	231.1756	24,307.85	49,421.97	103,282.74	1.2440	1.6800	2.4100
	Combined forecasting system	−0.1579	−1.2456	−1.1114	50.4318	79.7675	118.2327	3847.20	10,580.42	23,714.55	0.5306	0.8335	1.2603
FRI.	BPNN	12.2858	11.5586	19.3356	82.8441	104.8186	142.5571	13,523.99	26,727.86	53,413.52	0.8365	1.0593	1.4524
	FABPNN	14.7240	15.6039	22.3312	87.5349	111.5343	156.4354	15,983.89	28,458.85	58,309.17	0.8845	1.1351	1.6003
	ENN	12.1283	9.7140	17.3316	101.8761	131.7470	170.1288	20,140.88	38,866.10	72,284.31	1.0334	1.3553	1.7397
	WNN	−4.3370	−22.6447	−4.8305	155.6390	198.0136	266.9812	69,985.41	102,668.91	207,077.15	1.6050	2.0628	2.7662
	Combined forecasting system	5.1834	8.8412	28.7141	43.1650	60.7125	100.7607	3316.25	7569.48	21,664.29	0.4429	0.6223	1.0342
SAT.	BPNN	15.5543	33.1097	48.4879	85.7014	113.2363	130.2246	17,019.51	26,498.77	33,826.42	0.9208	1.2238	1.4201
	FABPNN	12.7572	30.7282	54.9176	91.6801	118.8509	135.0957	19,685.11	29,051.83	35,875.16	0.9865	1.2921	1.4751
	ENN	8.9360	27.6970	69.9136	104.2473	144.1342	157.3298	26,924.21	42,076.42	51,964.64	1.1198	1.5648	1.7123
	WNN	5.3048	17.9823	55.9119	119.7350	165.8653	194.2388	33,275.56	55,086.71	77,887.75	1.2868	1.7943	2.1188
	Combined forecasting system	−1.9062	2.6399	−7.8381	46.3772	63.6460	114.9571	3754.72	8630.02	33,023.62	0.5052	0.6898	1.2506
SUN.	BPNN	12.1084	13.4068	16.6830	93.6335	131.9624	164.3304	15,544.89	35,966.09	55,245.02	1.0496	1.4683	1.8586
	FABPNN	9.4427	9.2576	14.3211	90.8458	130.7386	150.0563	14,898.63	33,837.19	46,475.60	1.0213	1.4608	1.6896
	ENN	7.7045	14.5853	32.2788	117.4224	162.3855	212.7786	26,470.69	54,663.72	90,407.86	1.3117	1.7975	2.3623
	WNN	−7.0600	−15.6229	−14.4743	135.7484	191.2429	248.3169	33,576.98	72,513.26	123,455.02	1.5239	2.1430	2.7985
	Combined forecasting system	3.4471	−4.2469	10.8028	46.7796	68.7158	101.1263	3391.82	8848.73	23,580.16	0.5332	0.7702	1.1393

Table 8. Improvement percentages generated by the combined forecasting system from June data.

Week		Combined Forecasting System vs. BPNN			Combined Forecasting System vs. FABPNN			Combined Forecasting System vs. ENN			Combined Forecasting System vs. WNN		
		1-Step	**2-Step**	**3-Step**	**1-Step**	**2-Step**	**3-Step**	**1-Step**	**2-Step**	**3-Step**	**1-Step**	**2-Step**	**3-Step**
MON.	ζ_{MAE}	38.7282	30.2196	24.7450	41.8318	33.7773	31.9939	50.4148	41.9319	38.0612	59.4249	52.9131	54.4283
	ζ_{MSE}	60.9242	55.1893	36.5412	66.5465	61.1267	48.8399	77.6445	74.8546	65.3841	85.8728	82.4540	81.9570
	ζ_{MAPE}	37.6519	31.5059	24.4726	40.3689	34.1403	31.1715	48.8846	42.5385	38.0085	58.3164	52.9574	53.4797
TUE.	ζ_{MAE}	23.6262	20.1635	12.0723	27.6239	22.2991	18.3152	45.8347	36.4028	29.5607	53.8657	47.4955	48.7342
	ζ_{MSE}	35.8308	39.9793	25.4931	46.5332	47.8125	35.1182	71.9310	70.8891	61.4235	79.8578	78.1704	77.9472
	ζ_{MAPE}	23.3009	19.7554	13.0928	26.8799	21.4272	19.2107	44.8495	36.0763	29.0718	53.1431	47.2518	49.0783
WED.	ζ_{MAE}	36.5347	24.8646	31.1391	36.2166	24.5877	31.7916	50.3640	43.0386	46.8078	65.9249	57.5456	61.7106
	ζ_{MSE}	64.5338	47.6529	52.1098	65.4383	49.4143	55.0481	79.9556	71.6758	74.6775	92.2658	85.0663	86.7337
	ζ_{MAPE}	34.8823	23.3265	28.9401	35.0988	23.6766	30.4738	49.1249	42.3050	45.4003	65.5392	57.3485	61.1882
THU.	ζ_{MAE}	39.1625	29.2018	21.8182	40.0329	28.3480	24.0773	51.7850	42.0773	41.4183	57.8550	50.3284	48.8559
	ζ_{MSE}	65.9334	54.5338	46.0990	66.1252	51.7182	46.1118	79.8961	72.1866	68.8240	84.1730	78.5917	77.0392
	ζ_{MAPE}	37.8899	28.5181	19.2756	38.6298	27.2544	21.5181	50.6458	41.7446	39.1567	57.3467	50.3883	47.7055
FRI.	ζ_{MAE}	47.8960	42.0785	29.3191	50.6882	45.5661	35.5896	57.6299	53.9174	40.7739	72.2659	69.3392	62.2593
	ζ_{MSE}	75.4787	71.6795	59.4404	79.2525	73.4020	62.8458	83.5347	80.5242	70.0290	95.2615	92.6273	89.5381
	ζ_{MAPE}	47.0586	41.2547	28.7937	49.9301	45.1731	35.3744	57.1434	54.0812	40.5519	72.4060	69.8308	62.6123
SAT.	ζ_{MAE}	45.8852	43.7937	11.7240	49.4141	46.4489	14.9069	55.5123	55.8425	26.9324	61.2668	61.6279	40.8166
	ζ_{MSE}	77.9387	67.4324	2.3733	80.9261	70.2944	7.9485	86.0545	79.4896	36.4498	88.7163	84.3337	57.6010
	ζ_{MAPE}	45.1301	43.6331	11.9339	48.7844	46.6150	15.2153	54.8811	55.9157	26.9623	60.7366	61.5560	40.9745
SUN.	ζ_{MAE}	50.0397	47.9278	38.4616	48.5066	47.4404	32.6078	60.1613	57.6836	52.4735	65.5395	64.0689	59.2753
	ζ_{MSE}	78.1805	75.3970	57.3171	77.2341	73.8491	49.2633	87.1865	83.8124	73.9180	89.8984	87.7971	80.8998
	ζ_{MAPE}	49.1983	47.5462	38.7030	47.7906	47.2734	32.5716	59.3493	57.1516	51.7731	65.0099	64.0597	59.2897

Table 9. Statistical MAPE values of June data from New South Wales.

Week		BPNN			FABPNN			ENN			WNN			Combined Forecasting System		
		1-Step	2-Step	3-Step	1-Step	2-Step	3-Step	1-Step	2-Step	3-Step	1-Step	2-Step	3-Step	1-Step	2-Step	3-Step
MON.	Minimum	0.8043	1.0825	1.2366	0.8942	1.1130	1.4995	0.9850	1.3292	1.5792	1.0627	1.3828	1.8189	0.5457	0.7561	1.1092
	Maximum	0.9856	1.3688	1.9419	1.0261	1.5091	2.3099	1.2692	1.7254	2.2685	2.6880	2.9717	4.7548	0.5957	0.9456	1.6676
	Mean	0.9174	1.2451	1.6564	0.9592	1.3014	1.8176	1.1190	1.4940	2.0180	1.3722	1.8197	2.6891	0.5720	0.8562	1.2510
	Std.	0.0569	0.1021	0.2331	0.0441	0.1234	0.2300	0.0808	0.0998	0.2260	0.4092	0.4189	0.7260	0.0152	0.0548	0.1365
TUE.	Minimum	0.5935	0.7241	0.9108	0.6255	0.8279	1.1066	0.9018	1.0463	1.1664	0.8322	1.0390	1.3940	0.4993	0.6988	0.9078
	Maximum	0.8542	1.1470	1.5677	0.9109	1.2244	1.4925	1.1213	1.4229	1.8940	1.5753	1.8114	2.8523	0.5820	0.8532	1.2966
	Mean	0.7028	0.9438	1.1964	0.7372	0.9622	1.2870	0.9774	1.1772	1.4659	1.1504	1.4342	2.0418	0.5390	0.7543	1.0397
	Std.	0.0743	0.1108	0.1890	0.0936	0.1134	0.1116	0.0599	0.0977	0.1834	0.2187	0.2220	0.3826	0.0265	0.0413	0.1148
WED.	Minimum	0.5241	0.7211	0.9437	0.5385	0.7347	1.1555	0.8101	1.1846	1.5087	0.8226	1.1076	1.6440	0.4281	0.6665	0.8328
	Maximum	0.8211	1.2069	1.5934	0.8591	1.2694	1.7192	1.0159	1.4252	2.0176	4.1377	4.3909	5.7335	0.4704	0.7955	1.2923
	Mean	0.6894	0.9568	1.3629	0.6917	0.9612	1.3910	0.8824	1.2715	1.7651	1.3027	1.7217	2.4934	0.4489	0.7336	0.9664
	Std.	0.0892	0.1437	0.1863	0.0972	0.1576	0.2001	0.0541	0.0644	0.1688	0.8169	0.7633	0.9842	0.0129	0.0340	0.1311
THU.	Minimum	0.6916	0.9481	1.1672	0.6737	0.9123	1.3060	0.9899	1.3060	1.7124	1.0509	1.3108	1.8042	0.4991	0.7503	1.0305
	Maximum	1.0146	1.3523	2.2435	0.9886	1.2857	1.8434	1.1688	1.5936	2.4102	1.8008	2.4480	3.3178	0.5863	0.9070	1.5658
	Mean	0.8543	1.1660	1.5612	0.8646	1.1457	1.6058	1.0751	1.4307	2.0714	1.2440	1.6793	2.4111	0.5306	0.8335	1.2603
	Std.	0.1020	0.1313	0.3072	0.0855	0.1159	0.1533	0.0510	0.0839	0.2123	0.1921	0.2765	0.3558	0.0223	0.0457	0.1396
FRI.	Minimum	0.5844	0.6814	0.9806	0.6386	0.8048	1.1689	0.9208	1.1742	1.4278	0.8704	1.1843	1.7069	0.4276	0.5480	0.8679
	Maximum	0.9892	1.2772	1.7613	1.2784	1.5289	2.2955	1.1001	1.5049	2.0556	6.7672	7.3196	7.3120	0.4639	0.6833	1.1764
	Mean	0.8365	1.0593	1.4524	0.8845	1.1351	1.6003	1.0334	1.3553	1.7397	1.6050	2.0628	2.7662	0.4429	0.6223	1.0342
	Std.	0.1296	0.1985	0.2332	0.1542	0.1966	0.3306	0.0525	0.0881	0.1335	1.5514	1.6569	1.5244	0.0098	0.0376	0.0884
SAT.	Minimum	0.7830	1.0670	1.1481	0.8194	1.0228	1.1172	1.0202	1.4331	1.4778	1.1211	1.5391	1.6387	0.4792	0.6332	1.0244
	Maximum	1.1444	1.5721	1.8496	1.1400	1.5249	2.1447	1.2005	1.7259	1.9487	1.8326	2.2039	2.9383	0.5381	0.7604	1.4706
	Mean	0.9208	1.2238	1.4201	0.9865	1.2921	1.4751	1.1198	1.5648	1.7123	1.2868	1.7943	2.1188	0.5052	0.6898	1.2506
	Std.	0.1246	0.1506	0.2028	0.0848	0.1567	0.2447	0.0549	0.0733	0.1507	0.1960	0.2133	0.3953	0.0161	0.0392	0.1528
SUN.	Minimum	0.8227	1.0935	1.2744	0.8200	1.1629	1.3323	1.1823	1.6308	2.0706	1.3185	1.8957	2.2049	0.5042	0.6573	0.9825
	Maximum	1.2592	1.7874	2.3666	1.2804	1.7811	2.1908	1.5200	2.1595	2.6689	2.1173	2.6635	3.4449	0.5683	0.8527	1.5572
	Mean	1.0496	1.4683	1.8586	1.0213	1.4608	1.6896	1.3117	1.7975	2.3623	1.5239	2.1430	2.7985	0.5332	0.7702	1.1393
	Std.	0.1528	0.2266	0.3622	0.1400	0.2065	0.2922	0.0843	0.1425	0.1899	0.2158	0.2316	0.3270	0.0202	0.0500	0.1751

Remark. *Based on the above experiment, the proposed forecasting system exhibits superior performance in all forecasting error indexes. Furthermore, the developed system achieves the smallest maximum and minimum MAPE values, which means that it displays superior capability among the investigated models. The developed forecasting system also achieves forecasting stability, because its MAPE Std. values are smallest. Therefore, the proposed combined forecasting system achieves forecasting accuracy and stability simultaneously. Moreover, we find that the combined forecasting system performs effectively in different month which can be safely conclude that the improved data preprocessing and modified SVM have great contribution to enhance the forecasting effectiveness of the proposed system. In summary, the proposed forecasting system has better forecasting performance and universal applicability which can be widely applied for load forecasting as well as other fields.*

4.2.3. Experiment III: Comparison with Benchmark Model

In this section, the ARIMA model is selected as a benchmark model for comparison with the developed combined forecasting system. The half-hour power load data from February and June are applied to contradistinguish the prediction performances of the developed combined forecasting system and ARIMA model. The average values of AE, MAE, MSE and MAPE for February and June are displayed in Table 10, where it is revealed that the combined forecasting system achieves lower MAPE values than the ARIMA model. To express prediction capability clearly, the comparison of prediction results for Wednesday in June, for the combined forecasting system and ARIMA model, are shown in Figure 8. From the results of Table 10 and Figure 8, we can conclude that the proposed nonlinear combined forecasting system can achieve better forecasting performance than ARIMA model.

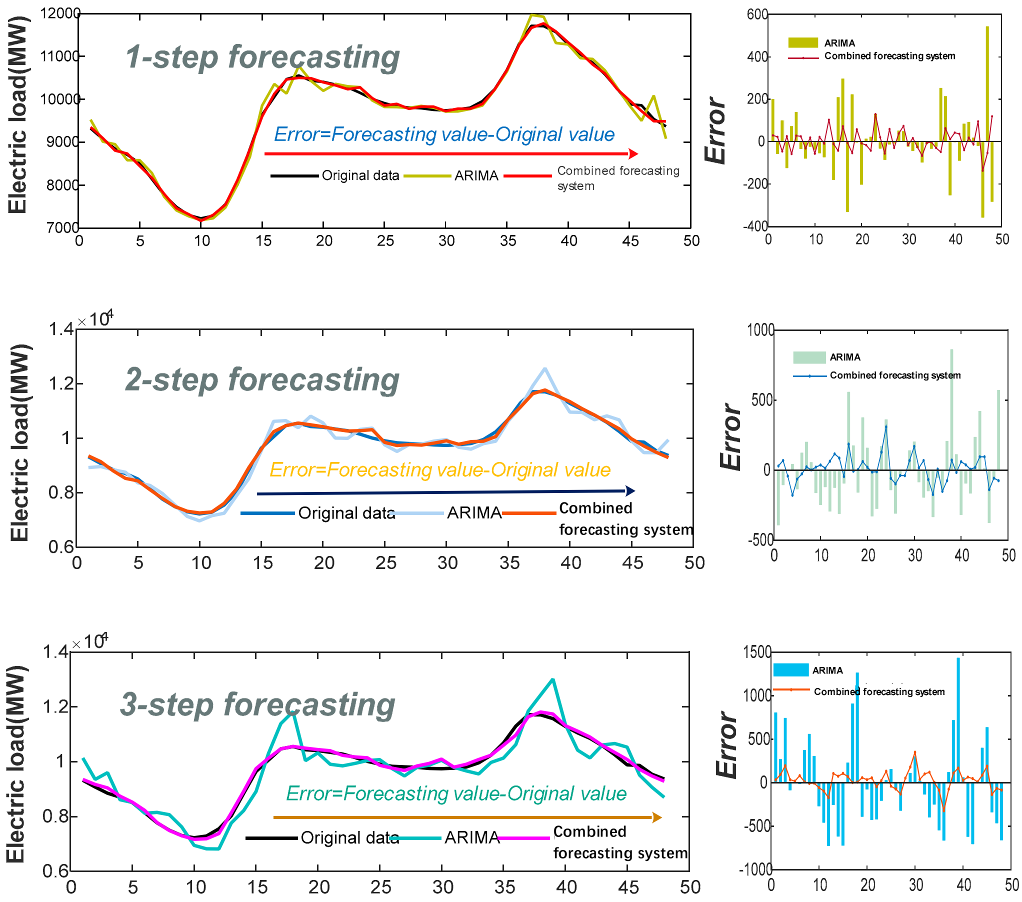

Figure 8. Comparison of 1-step to 3-step forecasting performance of the proposed combined forecasting system and ARIMA model.

Table 10. Forecasting results of the proposed combined forecasting system and ARIMA model.

	AE			MAE			MSE			MAPE		
	1-Step	**2-Step**	**3-Step**	**1-Step**	**2-Step**	**3-Step**	**1-Step**	**2-Step**	**3-Step**	**1-Step**	**2-Step**	**3-Step**
February												
ARIMA	0.4733	5.1282	2.3802	116.3646	168.6304	239.2805	23,001.97	52,536.41	92,779.14	1.3620	1.9657	2.8060
Combined forecasting system	−5.2888	−4.4512	−13.9419	45.8323	66.3317	101.1104	3477.41	8503.16	18,967.24	0.5459	0.7786	1.1918
June												
ARIMA	−0.2541	8.4307	14.9222	139.1223	236.8844	397.5834	36,617.72	101,576.84	279,856.30	1.4511	2.4757	4.1315
Combined forecasting system	2.9225	4.7050	5.2594	47.9674	71.4195	107.2645	3828.36	9193.13	23,974.01	0.5103	0.7514	1.1345

4.3. Summary

Based on experiments I–III, we conclude that:

(a) For 1-step to 3-step forecasting, the developed combined forecasting system achieves smaller values for all forecasting error metrics than the single models. In addition, the developed combined forecasting system also obtains the lowest MAPE Std. results. Overall, through improved data preprocessing method and modified SVM, the developed system is superior to the four single models in terms of both validity and stability.
(b) The developed combined forecasting system achieves lower MAPE results than the benchmark ARIMA model in 1-step to 3-step forecasting. Therefore, we can conclude that the developed combined forecasting system outperforms the ARIMA model in electrical load forecasting.
(c) Compared with the individual prediction models, the predictive ability of the developed combined forecasting system exhibits significant improvements. According to relevant literature [3], if the electrical load forecasting error were to decrease by 1%, the operating costs would decrease by 10 million pounds. Consequently, considerable economic benefit could be generated.

5. Discussion

An insightful discussion based on above case studies is conducted in this section, which can provide detailed and comprehensive analysis for the experimental results.

5.1. Discussion of the Significance of the Developed Forecasting System with Testing Method

DM test and forecasting effectiveness are used as two testing method to demonstrate the capability of the developed forecasting system.

(a) Table 11 presents the DM statistics, where the square error loss function values are applied, and demonstrates that the combined forecasting system differs from BPNN, FABPNN, ENN, WNN and ARIMA at the 1% significance level in multi-step forecasting.
(b) Table 11 implies the one-order and two-order forecasting effectiveness of the developed forecasting system and other compared models. From Table 11, it can be determined that the proposed forecasting system obtains the largest value of forecasting effectiveness compared with other compared models in multi-step forecasting.

Remark. *From the results of the DM test and forecasting effectiveness, we can conclude that the developed nonlinear combined forecasting system exhibits superior forecasting performance to the other models and the prediction validity of the developed forecasting system and others differs significantly.*

Table 11. Results for the DM test and the forecasting effectiveness.

Test Method	Average Value	1-step	2-step	3-step
DM-test	BPNN	2.9934 ***	2.8608 ***	2.6476 ***
	FABPNN	2.9884 ***	2.8418 ***	2.7172 ***
	ENN	3.3992 ***	3.1337 ***	2.9694 ***
	WNN	3.7132 ***	3.3533 ***	3.3633 ***
	ARIMA	3.8003 ***	3.4451 ***	4.0389 ***
	Average Value	**1-step**	**2-step**	**3-step**
Forecasting effectiveness [1]	BPNN	0.9913	0.9879	0.9851
	FABPNN	0.9913	0.9878	0.9853
	ENN	0.9895	0.9857	0.9824
	WNN	0.9885	0.9843	0.9796
	ARIMA	0.9859	0.9778	0.9653
	Combined forecasting system	0.9948	0.9925	0.9899
	Average Value	**1-step**	**2-step**	**3-step**
Forecasting effectiveness [2]	BPNN	0.9838	0.9770	0.9713
	FABPNN	0.9836	0.9770	0.9717
	ENN	0.9801	0.9724	0.9659
	WNN	0.9787	0.9703	0.9616
	ARIMA	0.9736	0.9584	0.9385
	Combined forecasting system	0.9906	0.9858	0.9804

*** Indicates the 1% significance level; [1] Indicates the one-order forecasting effectiveness; [2] Indicates the two-order forecasting effectiveness.

5.2. Discussion of Comparison with Linear Combined Models

To further validate the effectiveness of the developed nonlinear combined forecasting system, two linear combined methods, which include the average value method and entropy weight method, are applied to compare with the proposed nonlinear combined forecasting system. More specifically, the average value method means that the weight of each individual model is equal to $1/M$ (M is the number of the individual models), and the entropy weight method calculated the weights of each single model by evaluating the amount of information of each individual model objectively.

To provide more detailed comparison information, the forecasting results of two randomly selected days (Saturday in February and Friday in June) are presented in Table 12. It is clearly revealed that the developed nonlinear combined forecasting system achieves lower MAPE values compared with the linear combined models in multi-step forecasting, indicating that the nonlinear combined forecasting system can provide more accurate forecasting result in engineering application.

Remark. *As demonstrated by the performances of the developed combined forecasting system and linear combined models, the developed combined forecasting system exhibits superior performance, indicating that improved data preprocessing and modified SVM can greatly enhance the performance of the nonlinear combined forecasting system in electrical load forecasting.*

5.3. Discussion of the Superiority of the Optimization Algorithm

To test the superiority of the optimization algorithm used in the developed forecasting system, the discussion of comparison with other typical optimization algorithm, i.e., FA, Ant lion optimizer (ALO) and Dragonfly algorithm (DA), is performed in this section. As shown in Figure 9, four typical test functions, including two unimodal test functions (i.e., Function 1 and Function 2) and two multimodal test functions (i.e., Function 3 and Function 4), are tested in this section. Figure 9 presents the curve of fitness value of the MFO and other compared algorithms, which is employed to validate the effectiveness of the MFO algorithm in terms of convergence performance. In brief, it can be observed that the MFO is better than that of other compared algorithms.

Table 12. Comparison between the proposed combined forecasting system and linear combined models.

	AE			MAE			MSE			MAPE		
	1-Step	**2-Step**	**3-Step**	**1-Step**	**2-Step**	**3-Step**	**1-Step**	**2-Step**	**3-Step**	**1-Step**	**2-Step**	**3-Step**
SAT.												
Average value method	30.4489	−63.6749	−61.5016	84.582	128.3602	149.4587	13,397.84	28,370.37	38,526.36	1.0156	1.5425	1.8083
Entropy weight method	29.3053	−62.6083	−59.9099	83.78	127.4186	147.9893	13,213.82	28,112.81	38,044.91	1.0044	1.5293	1.7879
Combined forecasting system	−9.9972	−15.8985	−16.938	42.2213	60.0048	97.4307	3253	7601.39	16,427.04	0.5115	0.726	1.1988
FRI.												
Average value method	8.7003	3.5579	13.542	83.3551	104.9405	142.5478	13,811.16	26,506.87	55,862.19	0.8416	1.0666	1.4595
Entropy weight method	8.9007	4.0851	13.8869	83.196	104.477	141.4894	13,779.77	26,349.11	55,349.16	0.8398	1.0618	1.4479
Combined forecasting system	5.1834	8.8412	28.7141	43.165	60.7125	100.7607	3316.25	7569.48	21,664.29	0.4429	0.6223	1.0342

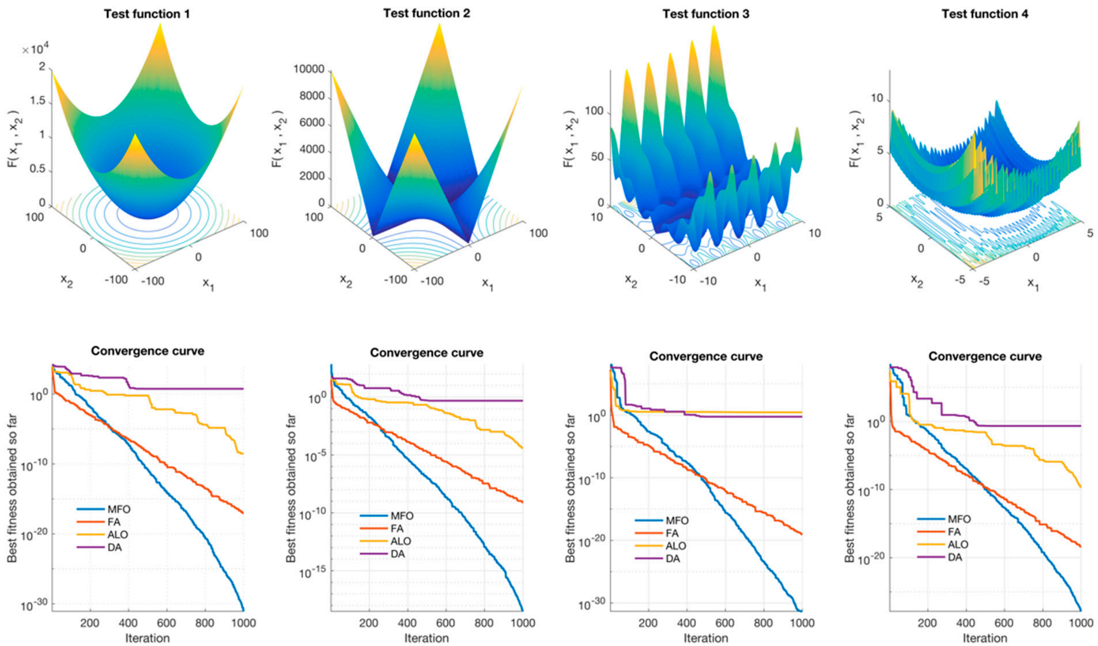

Figure 9. Comparison of the curve of fitness value of the MFO and other compared algorithms.

Remark. *According to the comparison of the MFO algorithm and other compared algorithms, the MFO algorithm shows superior performance, indicating that the MFO algorithm can provide very promising and competitive optimization results, which further illustrates that the MFO algorithm can contribute greatly to the excellent performance of the developed forecasting system.*

5.4. Further Validation for the Stability of the Developed Combined Forecasting System

Although the statistical MAPE values presented in Tables 6 and 9 well evaluate the stability of the developed forecasting system, to prove the effectiveness and applicability, further validation needs to be conducted by another method. Therefore, based on the performance variance used in [57], the standard deviation of forecasting errors is employed to verify the stability of the developed combined forecasting system. As demonstrated in Table 13, the standard deviation values of the proposed forecasting system are smaller than other compared models, indicating that the developed forecasting system is more stable than other comparison models.

Table 13. Results for the standard deviation of forecasting errors.

Average Value	1-Step	2-Step	3-Step
BPNN	103.0949	141.1311	177.1506
FABPNN	104.3878	140.8473	175.7578
ENN	127.8786	174.4013	217.9661
WNN	132.0079	178.8134	236.4214
ARIMA	172.1966	274.8526	416.6033
Combined forecasting system	58.8549	89.8436	124.6596

Remark. *The results for the standard deviation of forecasting errors also account for the conclusion obtained from Tables 6 and 9, i.e., the developed combined forecasting system is superior to all considered compared models in terms of stability. In summary, we can conclude that both the accuracy and stability of the developed forecasting system performs better than all considered compared models.*

6. Conclusions

Electrical load forecasting plays a considerably significant role in power systems. More accurate forecasting results are vital for economic operation and provide more valid information for decision makers. Therefore, conducting accurate forecasting of electrical loads appears to be particularly important to reduce costs and risks. However, it is difficult to achieve desirable performance using single methods. The combined method can sufficiently incorporate the advantages of individual models; however, the application of linear combinations is limited because the possibility of nonlinear terms is ignored. Therefore, in this study, a novel nonlinear combined forecasting system, which consists of three modules (improved data pre-processing module, the forecasting module, and the evaluation module) is developed for electric load forecasting which successfully overcomes the drawbacks that existed in linear combined forecasting models. Different from the simple data pre-processing of most previous studies, the improved data pre-processing module based on longitudinal data selection is successfully developed in this system, which further improves the effectiveness of data pre-processing and then enhances the final forecasting performance. Moreover, the modified support vector machine is developed to integrate all the individual predictors and obtain the final prediction, which successfully overcomes the upper drawbacks of the linear combined model. Furthermore, the evaluation module is incorporated to perform a scientific evaluation for the developed system.

According to the experimental results and analyses, the developed forecasting system exhibits a more precise prediction capability than the four single models. For example, in 1-step prediction, the average MAPE values of the developed forecasting system, BPNN, FABPNN, ENN and WNN are 0.5281%, 0.9411%, 0.9581%, 1.1011% and 1.5047%, respectively; in 2-step prediction, the average MAPE values are 0.7650%, 1.2889%, 1.3036%, 1.4834% and 2.0018%, respectively; and in 3-step forecasting, the average MAPE values of the five models are 1.1631%, 1.6619%, 1.6800%, 1.8781% and 2.6247%, respectively. Furthermore, the proposed forecasting system obtains the lowest MAPE Std. results, indicating that it can maintain stability in electrical load forecasting. The results of the DM test and forecasting effectiveness confirm the evidence that the developed nonlinear combined forecasting system outperforms the single models and ARIMA benchmark model. Furthermore, the proposed combined forecasting system exhibits effective prediction ability compared to the linear combined models. In summary, the developed combined forecasting system, which has excellent properties, is a promising model for power load forecasting as well as other fields.

Acknowledgments: This research was supported by the Major Program of National Social Science Foundation of China (Grant No. 14ZDB130).

Author Contributions: Chengshi Tian proposed the concept of this research and provided overall guidance, Yan Hao wrote the whole manuscript, and carried on data analysis.

Conflicts of Interest: The authors declare no conflict of interest.

References

1. Quan, H.; Srinivasan, D.; Khosravi, A. Uncertainty handling using neural network-based prediction intervals for electrical load forecasting. *Energy* **2014**, *73*, 916–925. [CrossRef]
2. Shu, F.; Luonan, C. Short-term load forecasting based on an adaptive hybrid method. *Power Syst. IEEE Trans.* **2006**, *21*, 392–401. [CrossRef]
3. Lee, C.-W.; Lin, B.-Y. Application of Hybrid Quantum Tabu Search with Support Vector Regression (SVR) for Load Forecasting. *Energies* **2016**, *9*, 873. [CrossRef]
4. Zjavka, L.; Snášel, V. Short-term power load forecasting with ordinary differential equation substitutions of polynomial networks. *Electr. Power Syst. Res.* **2016**, *137*, 113–123. [CrossRef]
5. Du, P.; Wang, J.; Yang, W.; Niu, T. Multi-step ahead forecasting in electrical power system using a hybrid forecasting system. *Renew. Energy* **2018**, *122*, 533–550. [CrossRef]
6. Yang, W.; Wang, J.; Wang, R. Research and application of a novel hybrid model based on data selection and artificial intelligence algorithm for short term load forecasting. *Entropy* **2017**, *19*, 52. [CrossRef]
7. The 12 Biggest Blackouts in History. Available online: http://www.msn.com/en-za/news/offbeat/the-12-biggest-blackouts-in-history/ar-CCeNdC#page=1 (accessed on 13 March 2018).
8. Wang, Y.; Wang, J.; Zhao, G.; Dong, Y. Application of residual modification approach in seasonal ARIMA for electricity demand forecasting: A case study of China. *Energy Policy* **2012**, *48*, 284–294. [CrossRef]
9. Huang, M.-L. Hybridization of Chaotic Quantum Particle Swarm Optimization with SVR in Electric Demand Forecasting. *Energies* **2016**, *9*, 426. [CrossRef]
10. Dudek, G. Pattern-based local linear regression models for short-term load forecasting. *Electr. Power Syst. Res.* **2016**, *130*, 139–147. [CrossRef]
11. Guo, Y.; Nazarian, E.; Ko, J.; Rajurkar, K. Hourly cooling load forecasting using time-indexed ARX models with two-stage weighted least squares regression. *Energy Convers. Manag.* **2014**, *80*, 46–53. [CrossRef]
12. Wang, X. Grey prediction with rolling mechanism for electricity demand forecasting of Shanghai. In Proceedings of the 2007 IEEE International Conference on Grey Systems and Intelligent Services, GSIS 2007, Nanjing, China, 18–20 November 2007; pp. 689–692.
13. Dong, Y.; Wang, J.; Wang, C.; Guo, Z. Research and Application of Hybrid Forecasting Model Based on an Optimal Feature Selection System—A Case Study on Electrical Load Forecasting. *Energies* **2017**, *10*, 490. [CrossRef]
14. Lee, C.M.; Ko, C.N. Short-term load forecasting using lifting scheme and ARIMA models. *Expert Syst. Appl.* **2011**, *38*, 5902–5911. [CrossRef]
15. Zhang, M.; Bao, H.; Yan, L.; Cao, J.; Du, J. Research on processing of short-term historical data of daily load based on Kalman filter. *Power Syst Technol.* **2003**, *9*, 39–42.
16. Lin, W.-M.; Gow, H.-J.; Tsai, M.-T. An enhanced radial basis function network for short-term electricity price forecasting. *Appl. Energy* **2010**, *87*, 3226–3234. [CrossRef]

17. Jain, R.K.; Smith, K.M.; Culligan, P.J.; Taylor, J.E. Forecasting energy consumption of multi-family residential buildings using support vector regression: Investigating the impact of temporal and spatial monitoring granularity on performance accuracy. *Appl. Energy* **2014**, *123*, 168–178. [CrossRef]
18. García-Martos, C.; Rodríguez, J.; Sánchez, M.J. Modelling and forecasting fossil fuels, CO2 and electricity prices and their volatilities. *Appl. Energy* **2013**, *101*, 363–375. [CrossRef]
19. Metaxiotis, K.; Kagiannas, A.; Askounis, D.; Psarras, J. Artificial intelligence in short term electric load forecasting: A state-of-the-art survey for the researcher. *Energy Convers. Manag.* **2003**, *44*, 1525–1534. [CrossRef]
20. Li, P.; Li, Y.; Xiong, Q.; Chai, Y.; Zhang, Y. Application of a hybrid quantized Elman neural network in short-term load forecasting. *Int. J. Electr. Power Energy Syst.* **2014**, *55*, 749–759. [CrossRef]
21. Liao, G.-C.; Tsao, T.-P. Application of fuzzy neural networks and artificial intelligence for load forecasting. *Electr. Power Syst. Res.* **2004**, *70*, 237–244. [CrossRef]
22. Dong, Y.; Ma, X.; Ma, C.; Wang, J. Research and application of a hybrid forecasting model based on data decomposition for electrical load forecasting. *Energies* **2016**, *9*, 50. [CrossRef]
23. Wang, J.; Yang, W.; Du, P.; Li, Y. Research and application of a hybrid forecasting framework based on multi-objective optimization for electrical power system. *Energy* **2018**, *148*, 59–78. [CrossRef]
24. Li, H.; Guo, S.; Zhao, H.; Su, C.; Wang, B. Annual electric load forecasting by a least squares support vector machine with a fruit fly optimization algorithm. *Energies* **2012**, *5*, 4430–4445. [CrossRef]
25. Peng, L.L.; Fan, G.F.; Huang, M.L.; Hong, W.C. Hybridizing DEMD and quantum PSO with SVR in electric load forecasting. *Energies* **2016**, *9*, 221. [CrossRef]
26. Wang, J.; Yang, W.; Du, P.; Niu, T. A novel hybrid forecasting system of wind speed based on a newly developed multi-objective sine cosine algorithm. *Energy Convers. Manag.* **2018**, *163*, 134–150. [CrossRef]
27. Wang, J.; Zhu, W.; Zhang, W.; Sun, D. A trend fixed on firstly and seasonal adjustment model combined with the ε-SVR for short-term forecasting of electricity demand. *Energy Policy* **2009**, *37*, 4901–4909. [CrossRef]
28. Osório, G.J.; Matias, J.C.O.; Catalão, J.P.S. Short-term wind power forecasting using adaptive neuro-fuzzy inference system combined with evolutionary particle swarm optimization, wavelet transform and mutual information. *Renew. Energy* **2015**, *75*, 301–307. [CrossRef]
29. Bates, J.M.; Granger, C.W.J. The Combination of Forecasts. *Oper. Res. Soc.* **1969**, *20*, 451–468. [CrossRef]
30. Wang, J.; Zhu, S.; Zhang, W.; Lu, H. Combined modeling for electric load forecasting with adaptive particle swarm optimization. *Energy* **2010**, *35*, 1671–1678. [CrossRef]
31. Xiao, L.; Wang, J.; Hou, R.; Wu, J. A combined model based on data pre-analysis and weight coefficients optimization for electrical load forecasting. *Energy* **2015**, *82*, 524–549. [CrossRef]
32. Zhao, W.; Wang, J.; Lu, H. Combining forecasts of electricity consumption in China with time-varying weights updated by a high-order Markov chain model. *Omega* **2014**, *45*, 80–91. [CrossRef]
33. Xiao, L.; Shao, W.; Liang, T.; Wang, C. A combined model based on multiple seasonal patterns and modified firefly algorithm for electrical load forecasting. *Appl. Energy* **2016**, *167*, 135–153. [CrossRef]
34. Li, M.W.; Han, D.F.; Wang, W. long Vessel traffic flow forecasting by RSVR with chaotic cloud simulated annealing genetic algorithm and KPCA. *Neurocomputing* **2015**, *157*, 243–255. [CrossRef]
35. Xu, Y.; Yang, W.; Wang, J. Air quality early-warning system for cities in China. *Atmos. Environ.* **2017**, *148*, 239–257. [CrossRef]
36. Hong, W.C.; Dong, Y.; Zhang, W.Y.; Chen, L.Y.; Panigrahi, B.K. Cyclic electric load forecasting by seasonal SVR with chaotic genetic algorithm. *Int. J. Electr. Power Energy Syst.* **2013**, *44*, 604–614. [CrossRef]
37. Chen, Y.; Hong, W.-C.; Shen, W.; Huang, N. Electric Load Forecasting Based on a Least Squares Support Vector Machine with Fuzzy Time Series and Global Harmony Search Algorithm. *Energies* **2016**, *9*, 70. [CrossRef]
38. Hong, W.C.; Dong, Y.; Lai, C.Y.; Chen, L.Y.; Wei, S.Y. SVR with hybrid chaotic immune algorithm for seasonal load demand forecasting. *Energies* **2011**, *4*, 960–977. [CrossRef]
39. Huang, N.; Shen, Z.; Long, S.; Wu, M.; Shih, H.; Zheng, Q.; Yen, N.; Tung, C.; Liu, H. The empirical mode decomposition and the Hilbert spectrum for nonlinear and non-stationary time series analysis. *Proc. R. Soc. A Math. Phys. Eng. Sci.* **1998**, *454*, 903–995. [CrossRef]
40. Fan, G.F.; Peng, L.L.; Zhao, X.; Hong, W.C. Applications of hybrid EMD with PSO and GA for an SVR-based load forecasting model. *Energies* **2017**, *10*, 1713. [CrossRef]

41. Fan, G.F.; Peng, L.L.; Hong, W.C.; Sun, F. Electric load forecasting by the SVR model with differential empirical mode decomposition and auto regression. *Neurocomputing* **2016**, *173*, 958–970. [CrossRef]
42. Fan, G.-F.; Qing, S.; Wang, H.; Hong, W.-C.; Li, H.-J. Support vector regression model based on empirical mode decomposition and auto regression for electric load forecasting. *Energies* **2013**, *6*, 1887–1901. [CrossRef]
43. Wu, Z.; Huang, N.E. Ensemble Empirical Mode Decomposition. *Adv. Adapt. Data Anal.* **2009**, *1*, 1–41. [CrossRef]
44. Torres, M.E.; Colominas, M.A.; Schlotthauer, G.; Flandrin, P. A complete ensemble empirical mode decomposition with adaptive noise. In Proceedings of the IEEE International Conference on Acoustics, Speech and Signal Processing (ICASSP), Prague, Czech Republic, 22–26 May 2011; pp. 4144–4147.
45. Zhang, W.; Qu, Z.; Zhang, K.; Mao, W.; Ma, Y.; Fan, X. A combined model based on CEEMDAN and modified flower pollination algorithm for wind speed forecasting. *Energy Convers. Manag.* **2017**, *136*, 439–451. [CrossRef]
46. Afanasyev, D.O.; Fedorova, E.A. The long-term trends on the electricity markets: Comparison of empirical mode and wavelet decompositions. *Energy Econ.* **2016**, *56*, 432–442. [CrossRef]
47. Chen, Y.; Yang, Y.; Liu, C.; Li, C.; Li, L. A hybrid application algorithm based on the support vector machine and artificial intelligence: An example of electric load forecasting. *Appl. Math. Model.* **2015**, *39*, 2617–2632. [CrossRef]
48. Vapnik, V.N. *The Nature of Statistical Learning Theory*; Springer: New York, NY, USA, 1995.
49. Vapnik, V.N. *Statistical Learning Theory*; Wiley: New York, NY, USA, 1998.
50. Ju, F.Y.; Hong, W.C. Application of seasonal SVR with chaotic gravitational search algorithm in electricity forecasting. *Appl. Math. Model.* **2013**, *37*, 9643–9651. [CrossRef]
51. Li, M.W.; Geng, J.; Wang, S.; Hong, W.C. Hybrid chaotic quantum bat algorithm with SVR in electric load forecasting. *Energies* **2017**, *10*, 2180. [CrossRef]
52. Liang, Y.; Niu, D.; Ye, M.; Hong, W.-C. Short-term load forecasting based on wavelet transform and least squares support vector machine optimized by improved cuckoo search. *Energies* **2016**, *9*, 827. [CrossRef]
53. Mirjalili, S. Moth-flame optimization algorithm: A novel nature-inspired heuristic paradigm. *Knowl.-Based Syst.* **2015**, *89*, 228–249. [CrossRef]
54. Zhao, H.; Zhao, H.; Guo, S. Using GM (1,1) Optimized by MFO with Rolling Mechanism to Forecast the Electricity Consumption of Inner Mongolia. *Appl. Sci.* **2016**, *6*, 20. [CrossRef]
55. Diebold, F.X.; Mariano, R.S. Comparing predictive accuracy. *J. Bus. Econ. Stat.* **1995**, *13*, 253–263. [CrossRef]
56. Chen, H.; Hou, D. Research on superior combination forecasting model based on forecasting effective measure. *J. Univ. Sci. Technol. China* **2002**, *2*, 172–180.
57. Wang, J.; Du, P.; Niu, T.; Yang, W. A novel hybrid system based on a new proposed algorithm—Multi-objective Whale Optimization Algorithm for wind speed forecasting. *Appl. Energy* **2017**, *208*, 344–360. [CrossRef]